Traffic-induced atmospheric pollution during the COVID-19 lockdown: Dispersion modeling based on traffic flow monitoring in Turin, Italy

Journal Pre-proof

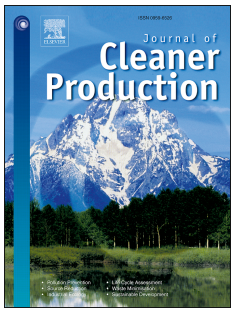

Traffic-induced atmospheric pollution during the COVID-19 lockdown: Dispersion modeling based on traffic flow monitoring in Turin, Italy

Marco Ravina, Zahra Shams Esfandabadi, Deborah Panepinto, Maria Chiara Zanetti

PII: S0959-6526(21)02637-8

DOI: https://doi.org/10.1016/j.jclepro.2021.128425

Reference: JCLP 128425

To appear in: *Journal of Cleaner Production*

Received Date: 1 February 2021

Revised Date: 20 May 2021

Accepted Date: 21 July 2021

Please cite this article as: Ravina M, Esfandabadi ZS, Panepinto D, Zanetti MC, Traffic-induced atmospheric pollution during the COVID-19 lockdown: Dispersion modeling based on traffic flow monitoring in Turin, Italy, *Journal of Cleaner Production* (2021), doi: https://doi.org/10.1016/j.jclepro.2021.128425.

Traffic-induced atmospheric pollution during the COVID-19 lockdown: dispersion modeling based on traffic flow monitoring in Turin, Italy

Marco Ravina*[,1], Zahra Shams Esfandabadi[1,2], Deborah Panepinto[1], Maria Chiara Zanetti[1]

[1] Department of Environment, Land and Infrastructure Engineering (DIATI), Politecnico di Torino, Corso Duca degli Abruzzi 24, 10129 Torino, Italy

[2] Energy center lab, Politecnico di Torino, Via Paolo Borsellino 38/16, 10138 Torino, Italy

** Corresponding author; Email: Marco.ravina@polito.it*

Abstract

The COVID-19 pandemic, as a worldwide threat to public health, has led many governments to impose mobility restrictions and adopt partial or full lockdown strategies in many regions to control the disease outbreak. Although these lockdowns are imposed to save public health by reducing the transmission of the virus, rather significant improvements of the air quality in this period have been reported in different areas, mainly as a result of the reduction in vehicular trips. In this research, the city of Turin in the northern part of Italy has been considered as the study area, because of its special meteorology and geographic location in one of the most polluted regions in

Europe, and also its high density of vehicular emissions. A Lagrangian approach is applied to illustrate and analyze the effect of imposing full lockdown restrictions on the reduction of traffic-induced air pollution in the city. To do this, the real-time traffic flow during the lockdown period is recorded, and by utilizing CALPUFF version 7, the dispersion of $PM_{2.5}$, Total Suspended Particulate (TSP), Benzo(a)pyrene (BaP), NO_x, and Black Carbon (BC) emitted from all circulating vehicles during and before the lockdown period are compared. Results indicate that the concentration of pollutants generated by road traffic sources (including passenger cars, busses, heavy-duty vehicles, light-duty vehicles, mopeds, and motorcycles) reduced at least 70% (for $PM_{2.5}$) up to 88.1% (for BaP) during the studied period. Concentration maps show that the concentration reduction varied in different areas of the town, mainly due to the characteristics and strength of the emission sources and the geophysical features of the area.

Keywords: Air quality, Dispersion Modeling, Emission, Pandemic, Transportation, Urban planning.

1. Introduction

The novel coronavirus-caused infectious disease 2019 (COVID-19), which was announced as a pandemic by the World Health Organization (WHO) on March 11, 2020 (WHO, 2020) has made a shock to the world and is turning into the largest threat to the public health worldwide in the 21st century (Chakraborty and Maity, 2020). To control the disease outbreak and flattening the epidemic curve, many regions have been imposing a partial or full lockdown in the highly infected areas. Although the lockdown restrictions were established to save public health by reducing the transmission of the virus, changes in the air and water quality in some areas (Ambade et al., 2021;

Muhammad et al., 2020; Saadat et al., 2020; Sharifi and Khavarian-Garmsir, 2020) have attracted the attention towards the environmental impacts of the pandemic lockdowns globally. In this regard, numerous research has been conducted on the changes in the air quality during the lockdown period in different countries across the globe, from China in the East (Griffith et al., 2020; Huang et al., 2020) to the United States in the West (Naeger and Murphy, 2020; Zangari et al., 2020), and some large areas such as western Europe (Menut et al., 2020). Besides, several pieces of research studied the potential link between the improvements in the air quality as a result of mitigating COVID-19 measures and the health benefits. These studies mainly concluded lower air pollution-related mortality due to less exposure to air pollution during this period (Gupta et al., 2020; Liu et al., 2021; Son et al., 2020). All these studies highlight the importance of air pollution control strategies to protect human health whether air pollutants increase the infection rate of COVID-19 or not (Cazzolla Gatti et al., 2020; Collivignarelli et al., 2021a; Dettori et al., 2020).

Air pollution, with its impacts both at the local and global scales, has caused many challenges and problems all around the world over the years (Izquierdo et al., 2020; Sivarethinamohan et al., 2020) such that concerns about this issue have been reflected in the 2030 Agenda for Sustainable Development adopted by the United Nations General Assembly (UN, 2015). The WHO has labeled air pollution as the major environmental threat to health (WHO, 2016) and has estimated that around 90% of the world population do not breathe the air complying with its Air Quality Guideline (WHO, 2005). Exposure to air pollutants leads to three million deaths per year (WHO, 2016), out of which 600,000 deaths happen among children less than five years of age (WHO, 2017). Such negative health impacts impose substantial economic costs to the societies (Chen and Chen, 2021; Stewart et al., 2017) and affect both humans and ecosystems (Panepinto et al., 2014). Therefore, in order to take steps towards clean air transitions, air quality action plans have been

considered as blueprints to achieve certain air quality objectives (Gross et al., 2019) by many countries all around the world, such as Spain (Izquierdo et al., 2020), China (Cai et al., 2017), the United Kingdom and the United States (Gross et al., 2019).

Air quality analysis and modeling in urban areas involve an inherent complexity (Pinto et al., 2020) due to the existence of a high number of air pollutant emission sources, the meteorological conditions of the region affecting the dispersion of the pollutants (Shen et al., 2021) and the chemical transformations of pollutants into secondary aerosols (EPA, 2015). However, air pollution dispersion models provide useful means to support decision-making in air quality control (Holnicki et al., 2016; Ravina et al., 2019) through estimating the concentration of pollutants in the atmosphere (Khan and Hassan, 2020). These deterministic mathematical models mostly follow Gaussian, Eulerian, or Lagrangian approaches (Liu et al., 2019), the Gaussian being a steady-state model and the two others being time-dependent (Khan and Hassan, 2020).

Dispersion models have been widely used for modeling the concentration of air pollutants in various case studies. In research conducted by Kesarkar et al. (2007), AERMOD, which is a steady-state Gaussian model, was utilized to model the dispersion of PM_{10} in Pune, India. Modeling the dispersion of PM_{10} was also conducted by Brusca et al. (2016) for the city of Turin, Italy, which is also the case study in the present research, by applying a 3D Computational Fluid Dynamics (CFD), coupling Eulerian and Lagrangian approaches. Omidi Khaniabadi et al. (2018) used the Gaussian SCREEN3 model and a Gaussian plume model to investigate the dispersion of fine particles including PM_{10}, $PM_{2.5,}$ and $PM_{1.0}$ related to a cement plant in Iran. Abdul-Wahab et al. (2017) considered a cement plant in Oman and used CALPUFF, as an advanced non-steady-state Lagrangian puff model, to model the dispersion of CO_2 emission. Moreover, Ravina et al.

(2018) used CALPUFF as a part of an integrated dispersion and externalities model to estimate the delta-concentration maps for NOx, $PM_{2.5,}$ and PM_{10} and calculate the health damage costs for the district heating system in the city of Turin. Selection among CALPUFF, SPRAY (which is a Lagrangian particle model), and AERMOD for modeling the pollutant dispersion is possible in the extended version of this integrated model (Ravina et al., 2020b).

Air pollution in urban areas is mainly linked with vehicular trips (Guttikunda et al., 2019; Pinto et al., 2020; Xiang et al., 2020). Therefore, the travel of various types of vehicles with different ages and fuel types on urban roads and streets adds more complication to the inherent complexity of the air quality modeling. However, air pollution dispersion models have also been used in the literature with a focus on traffic-induced air pollution. For instance, in the Tehran Metropolitan in Iran, which is struggling with air pollution as a major problem, Shahbazi et al. (2017) studied the impact of the traffic emission reduction plans on the concentration of CO and NO_x in the city by using Comprehensive Air Quality Model with Extensions (CAMx) that is an Eulerian photochemical model. Also, Shahbazi and Hosseini (2020) used CAMx to investigate the concentration of CO, NO_2, O_3, $PM_{2.5}$, $SO_{2,}$ and Black Carbon (BC) in Tehran in a highly polluted period in December 2017. Furthermore, considering the high level of traffic-related pollution in the metropolitan area of Madrid, Spain, and the Air Quality and Climate Change Plan launched by the city council to tackle air pollution issues, Izquierdo et al. (2020) used an Eulerian chemical-transport model called Community Multiscale Air Quality (CMAQ) to evaluate the outcome of implementing this plan regarding the concentration levels of $PM_{2.5}$, NO_2 and O_3 in the city. In another research, Borge et al. (2018) also used CMAQ to assess the traffic-related NO_2 emissions based on a short-term action plan in the city of Madrid. Applying CALPUFF, Abdul-Wahab and

Fadlallah (2014) and Charabi et al. (2018) studied the concentration of CO, NOx, and CO_2 resulting from traffic in two different areas in Oman.

The lockdowns imposed by the governments to control the spread of COVID-19 highly impacted the transportation sector in all countries (Gualtieri et al., 2020; Ranjbari et al., 2021), and therefore, rather significant improvements in the air quality in this period have been reported in many areas (Chen et al., 2021; Gautam, 2020; Wang et al., 2020; Xiang et al., 2020). However, Le et al. (2020) highlighted the unexpected air pollution in northern China during the COVID-19 lockdown period, which happened despite up to 90% reduction of certain emissions from various sources in this period. Improvements in the air quality have also been observed in Italy (Deserti et al., 2020a, 2020b), with an average of 48-60% reduction in road traffic leading to a significant reduction in NO_2 levels (Gualtieri et al., 2020). Collivignarelli et al. (2021b) studied the impact of the pandemic on the concentration of NO_2 in three megacities of London, Milan, and Paris, highlighting the role of traffic restrictions on the reduction of NO_2 concentration in these cities.

Although Xiang et al. (2020) showed that considering meteorological conditions plays a significant role in concluding the impacts of the pandemic on the traffic-induced air pollution levels within the cities, to the best of the authors' knowledge, no study has utilized air pollution dispersion models to study the changes in the concentration of air pollutants during the COVID-19 pandemic lockdown mainly focusing on the changes in urban transportation activities, yet. This is while some pieces of research are available on the analysis of the impact of COVID-19 restrictions on the changes in the traffic-related air pollution considering meteorological conditions from the lens of statistical analysis (Chen et al., 2021; Rossi et al., 2020; Xiang et al., 2020). Furthermore, as stated by Gualtieri et al. (2020), most of the studies focusing on the implications

130 of COVID-19 lockdowns for the urban air quality lack quantification of the changes in road mobile
131 sources during the lockdown restrictions.

132 Therefore, to fill the existing gap, the present research aims at applying a Lagrangian approach
133 to illustrate and analyze the role of traffic in the city of Turin, Italy, on the air quality of the city
134 during the lockdown period. This is done by comparing the emission of NO_2, Benzo(a)pyrene
135 (BaP), $PM_{2.5}$, Total Suspended Particulate (TSP), and BC from all traffic mobile sources in the
136 city during normal days and the COVID-19 country lockdown period based on the real-time traffic
137 flow data recorded in this period. Since the first pandemic lockdown and mobility restrictions in
138 Italy led to 42% fewer daily trips (Cartenì et al., 2020), modeling the dispersion of traffic-induced
139 pollutants before and during the lockdown period can provide useful insight into the role of mostly
140 unnecessary traffic in polluting the atmosphere in this city.

141 The remainder of the paper is structured as follows. Section 2 introduces the study area and
142 provides an overview of the research method applied, and the data gathered. Sections 3 presents
143 the results and section 4 provides a discussion and analysis on the maps illustrating the
144 concentration of pollutants before and during the lockdown period. Finally, section 5 concludes
145 the key findings of the paper on the changes in the concentration of air pollutants during the
146 COVID-19 pandemic lockdown, which are attributed to the changes in vehicular transportation
147 activities.

148

2. Materials and Method

2.1. Description of the study area

This research considers the city of Turin as the study area for two main reasons: (1) its special meteorological and geographic condition in Po Valley, which is one of the most polluted regions in Europe both in summer and winter (Deserti et al., 2020a); and (2) its high density of vehicular emissions, which is among the highest in Europe (Padoan et al., 2018).

Turin, the capital of the Piedmont region, is a highly industrialized city and densely populated metropolitan area, enjoying a humid subtropical climate. Being known as one of the most technological industrial centers in Europe, this city is located in the western end of the Po Valley, one of the most polluted areas in Europe in the northern part of Italy (Bono et al., 2016; Deserti et al., 2020a). The city suffers from the low dispersion of pollutants, since it is surrounded by the Alps and hills in the North, West, and East, and the wind speed in this area is low. Therefore, the air quality standards are not met in this city (Padoan et al., 2018), and the air quality of Turin is put among the worst in Europe (Sicard et al., 2020).

Research shows that the individual particles of atmospheric PM in Turin are small enough to enter the deep zones of the resident's lungs and cause serious health problems for them (Malandrino et al., 2016). Road traffic is one of the most important sources of pollutant emissions in Turin, owning the following share of the total concentration in the city: 40% of the PM_{10}, 30% of the $PM_{2.5}$, and 75 - 77% of NO_2 (Padoan et al., 2018; Piedmont Region, 2018). The motorization rate in Turin is around 615 per 1000 inhabitants (Kyoto-Club, 2019), leading to a high car density in this city. Therefore, studying the role of traffic in the emission of air pollutants is of high importance in this region.

2.2. Data

2.2.1. Traffic flow

The traffic flow data considered in the current research refers to two time periods before and during the first COVID-19 lockdown in the city of Turin. The pre-lockdown flow data were taken from the standard hourly mean flows for the year 2018 provided by 5T S.r.l., a company working in the areas related to traffic management in Turin. For the full lockdown period, the real-time traffic flow reported continuously by the real-time traffic monitoring of the 5T website (http://opendata.5t.torino.it/get_fdt) was recorded from March 9th to May 18th, 2020, representing the lockdown period. The recording was conducted with a frequency of 10 minutes and then, mean hourly flow was calculated and used for the analysis. The real-time traffic monitoring network in Turin is based on 31 traffic sensors, however, not all these sensors are properly transmitting data. Therefore, in this study, the analysis is restricted to 15 monitoring points, which effectively report data. Although this traffic monitoring network reports average vehicle speed in every road branch, speed data were not employed in the present study, due to low accuracy. For both the pre-lockdown and full lockdown periods, the available data reported total traffic flow, which was subsequently disaggregated based on circulating vehicle categories.

2.2.2. Vehicle type share

44 categories of circulating motor vehicles were identified for Turin, considering the class of vehicles in the city and the type of fuel they consume. These categories include busses (consuming

192 diesel, CNG, or electricity), heavy-duty and light-duty vehicles (consuming conventional or Euro
193 1-6 standard petrol), mopeds and motorcycles (consuming conventional or Euro 1- 3^{+} standard
194 petrol), and passenger cars (consuming electricity, or any conventional or Euro 1-6 standard diesel,
195 LPG or petrol).

196 The shares of vehicles before the lockdown were estimated based on the total number of
197 registered vehicles in each category in the city extracted from Automobile Club d'Italia
198 (http://www.aci.it/), and the hourly flow extracted from a report by 5T S.r.l. on vehicular mobility
199 in the Piedmont region (5T and Regione_Piemonte, 2019). For the lockdown period, the share of
200 each category in the hourly traffic flow in both working and non-working days was considered in
201 the simulation. Since no data on the share of each of the 44 specified categories in the hourly traffic
202 flow of Turin was available, and this type of data could not be extracted from the recorded traffic
203 flow, an estimation for the share of these vehicles in the traffic flow was made. The data regarding
204 the circulating vehicles was estimated based on the average number of kilometers traveled, and the
205 data regarding the registered vehicles were considered in order to verify the consistency of the
206 disaggregation into categories.

207

208 2.2.3. Emission factors

209 Traffic-induced emissions of NO_x, BaP, $PM_{2.5}$, TSP, and BC were considered in this research.
210 The emission factors of these pollutants, except for BC, for each of the specified 44 categories of
211 vehicles were extracted from the EMEP/EEA air pollutant emission inventory guidebook 2019
212 (http://efdb.apps.eea.europa.eu/). The emission factors for BC were extracted from Krecl et al.

(2017) for HDVs, from Ježek et al. (2015) for LDVs and motorbikes, and from Zavala et al. (2017) for buses. Emission factors for electricity consumption were considered zero. These factors are reported in Table A1 in Appendix A with a description of the vehicle categories and the average share of total traffic flow in Turin.

Total daily pollutant emission was calculated considering the average hourly share of vehicle flow for each of the 44 categories. For each hour and each road source, daily pollutant emission flow of a generic pollutant P was calculated based on Equation (1),

$$P = \sum_{i} \sum_{j} \sum_{h} F_{i,j,h}\, L_i\, EF_{P,j} \qquad (1)$$

where $F_{i,j,h}$ is the traffic flow in road i for vehicle category j at hour h (vehicles h^{-1}); L_i is the length of the road (m), and $EF_{P,j}$ is the average emission factor of the vehicle category j in terms of the pollutant P ($g\ km^{-1}\ vehicle^{-1}$).

2.2.4. Meteorology

Meteorological data were collected from three different meteorological stations in Turin, which are managed by the Local Environmental Protection Agency (ARPA) of the regional air pollution service of Piedmont Region (Figure 1). Hourly observations at the ground level of air humidity, precipitation, solar radiation, temperature, atmospheric pressure, wind speed, and wind direction were collected for this research. The radiosoundings from the WMO station of Milano Linate Airport, which is located approximately 150 km east of Turin, were considered for the collection of the required upper-air data (http://weather.uwyo.edu/). Although this station is rather

far from Turin, it is the only source of data in this regard and its soundings can be used considering the relative morphological homogeneity of the western part of the Po Valley (Calori et al., 2006) in which Turin is located. Weather observations were first processed with the CALMET model and then were fed into CALPUFF to conduct the dispersion modeling.

2.3. Dispersion modeling

In this study, the dispersion of pollutants was simulated using the CALPUFF modeling system. CALPUFF is a Lagrangian multi-layer, multi-species, non-steady-state puff dispersion model that simulates the effects of time- and space-varying meteorological conditions on pollution transport, transformation, and removal (US EPA, 2011). This model simulates puffs of the materials emitted from the modeled sources, reproducing dispersion and transformation processes along the way. Temporal and spatial variations in the meteorological fields are explicitly incorporated in the resulting distribution of puffs throughout a simulation period.

With the release of CALPUFF version 7, the linear sources have been replaced with road sources. A new module for representing roadway emissions in dispersion model simulations has been implemented. The new approach simulates line sources such as roadways using the concept of rod-like puffs. Emitting rods follow the same rules as emitting horizontally symmetric Gaussian puffs, but far fewer rods aligned with road segments are needed to emulate the uniform distribution of emissions along a road segment. Near-field “hot spots” can be resolved as well as the drift of pollutants to sensitive areas further away. . For more technical details on the CALPUFF model structure, see the user’s guide (Exponent, 2019; US EPA, 2011).

Simulations were conducted on a domain of 16.6 km × 14.6 km, with 10 vertical layers and a 100 m grid step. A total number of 2,484 road sources was considered in the simulation. Figure 1 illustrates the modeling domain, the road sources, and the measuring points of traffic flow in the city. A height of 1.5 m was assigned to the emission sources, which are the circulating vehicles categorized in each of the 44 specified classes. The detailed setting of simulation parameters is reported in Table A4 of Appendix A. Due to the high number of emission sources, the computational time required for the detailed simulation was high and therefore, the period of the simulation was restricted to one week, i.e. from April 12nd to April 19th, 2020, with hourly time resolution. No chemical transformation scheme was adopted in the simulations.

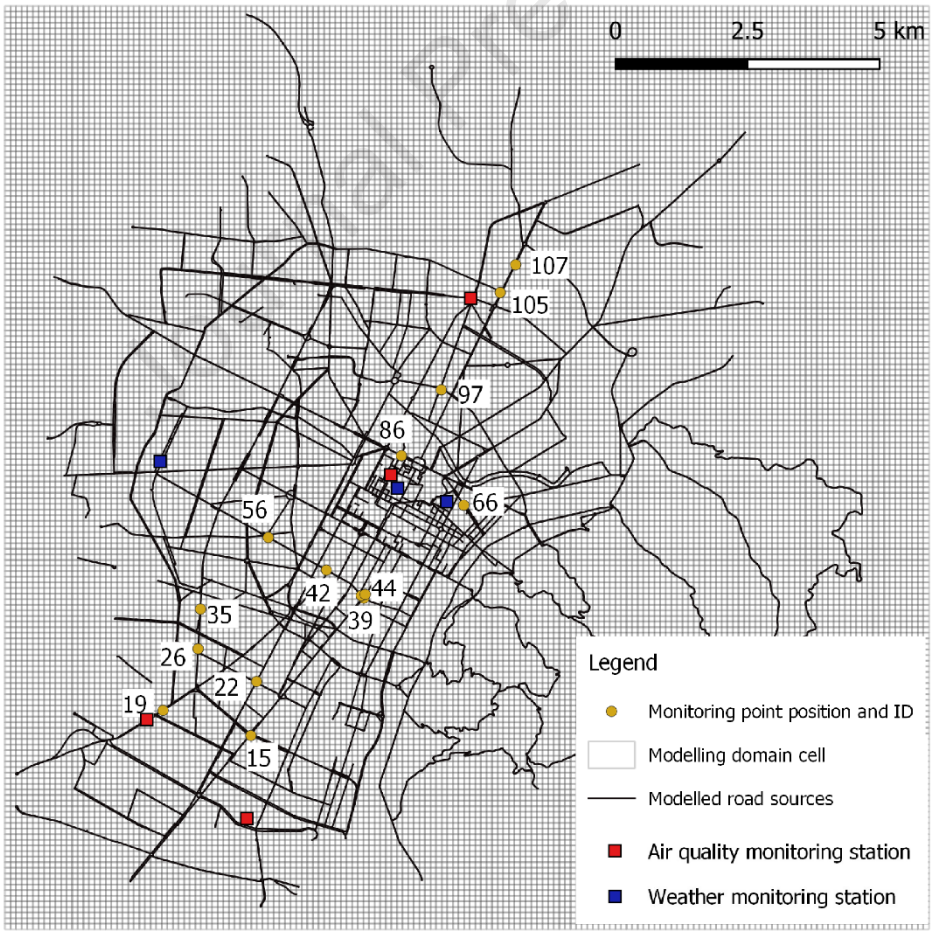

Figure 1. The modeling domain, the road graph, and the location of the monitoring stations.

The output concentrations were averaged over the observation period with the CALPOST processor and represented in the form of maps. Concentration maps of normal days and the COVID-19 country lockdown period were compared, and the reduction of pollutant concentration was calculated. NO_x to NO_2 conversion was modeled in CALPUFF using the MESOPUFF II scheme (Scire et al., 1984). Hourly ozone background concentrations recorded at the Turin Lingotto monitoring station were provided as input to the model.

3. Results

3.1. Traffic flow

Average real-time traffic flow in each hour of the day during the lockdown is compared with the average flow in a normal period, and the flow reduction during the working and non-working days are reported in Tables 2A and 3A in Appendix A, respectively. The same tables also report the average and standard deviation of the traffic flow reduction in each point and each hour of the day. During the working days, 69-88% reduction has been observed in the traffic monitoring points considered. If different hours of the day are examined, traffic flow reduction ranges from 66% to 96% during the day. Furthermore, during the non-working days, 74-92% reduction has been perceived in the studied monitoring points. If considering different hours of the day, a range of 49-99% is recognized for the reduction in traffic flow.

3.2. Pollutants emission and dispersion

The average traffic flow F in each road source during the COVID-19 lockdown days was calculated by scaling the flow in normal days for the average hourly flow reduction observed in the 15 monitoring points reported in Tables A2 and A3 in Appendix A. The results are reported in Table 1 and show an emission reduction between 71.4% ($PM_{2.5}$, working days) and 85.5% (BaP, non-working days).

Table 1. Daily pollutant emissions of Turin road traffic in normal days and during the COVID-19 lockdown.

Pollutant	Daily emission in normal working days (kg/d)	Daily emission during the lockdown working days (kg/d)	Emission Reduction (working days) (%)	Daily emission in normal non-working days (kg/d)	Daily emission during the lockdown non-working days (kg/d)	Emission Reduction (non-working days) (%)
NO_x	4,501	1,259	72.0	2,404	383	84.0
BaP	6E-03	1.6E-03	73.3	3.8E-03	5.5E-04	85.5
$PM_{2.5}$	114	32.5	71.4	65	11.1	82.9
TSP	621	174	72.0	337	54.3	83.9
BC	45.4	12.2	73.1	23.7	3.45	85.4

During the simulation period, there was no rainfall in Turin, except on April 19th, when a total amount of 1.6 mm of rain was recorded. The temperature and solar radiation, and wind distribution during this period are also presented in Figure 2. The wind rose in this figure shows two prevailing wind typologies, which are typical of the area and the period considered. One of them includes moderate winds (2 – 5 m/s) typically occurring during daytime with prevailing direction NE, and the other includes low winds (0 – 2 m/s) typically occurring during nighttime with prevailing direction SE.

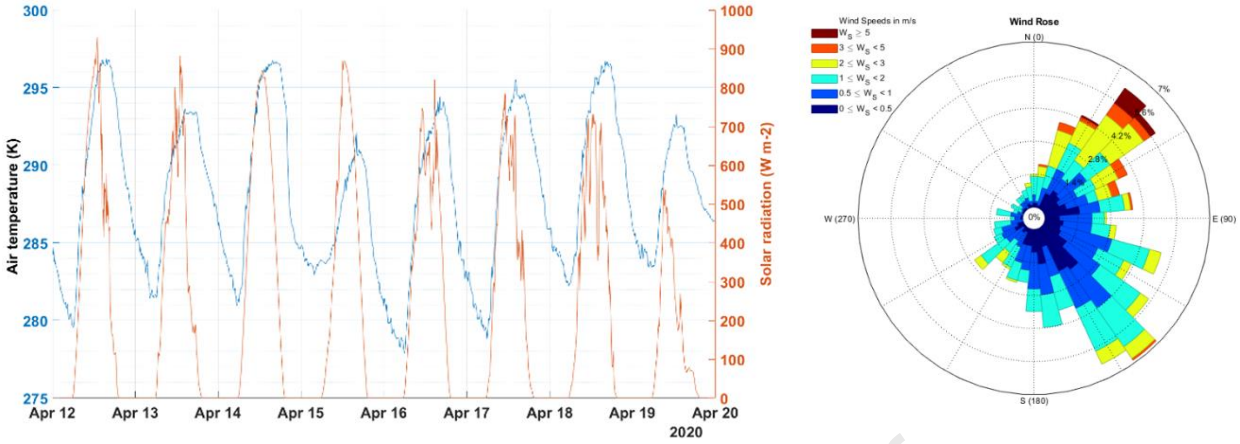

299 *Figure 2. Temperature and solar radiation (left) and wind distribution (right) in Turin during April 12-19, 2020*

300

301 Figure 3 displays the distribution of the atmospheric stability class, and the height of the mixed
302 layer, and Monin-Obukhov length (L_{mo}) during the simulated period. According to this figure,
303 stable (class F with a share of 33% and E with 12%) and unstable (class B with 32%) conditions
304 were prevailing, while neutral conditions (class C with 12% and D with 5%) were less frequent.
305 This trend is consistent with the general conditions observed during this period. Positive L_{mo} and
306 limited height of the mixed layer on April 14th, 15th, and 17th indicate that stable atmospheric
307 conditions were prevailing on these days, while negative L_{mo}values observed on the other days
308 show the prevalence of unstable conditions, in particular during the daytime.

309

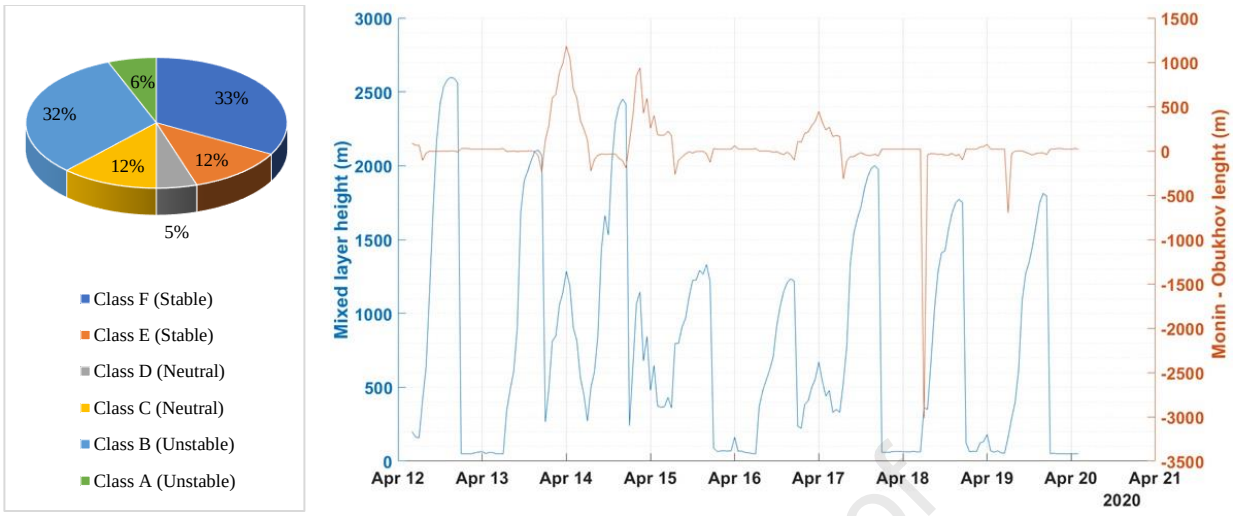

310 *Figure 3. Distribution of the atmospheric stability class (left) and height of the mixed layer and Monin-Obukhov*
311 *length (L_{mo}) (right) in Turin during April 12-19, 2020.*

312

313 Considering the average traffic flow before and during the lockdown, the share of each type of
314 vehicle from the flow, and the meteorological conditions during the studied period, the average
315 pollutant concentration maps are reported in Figure 4 to Figure 8. In these maps, pollutant
316 concentrations generated by urban road traffic on normal days are compared with those generated
317 during one week of the COVID-19 lockdown (April 12nd to April 19th, 2020) based on the same
318 meteorological conditions. The average concentration reduction is reported in Table 2 and finally,
319 presented in Figure 9.

320

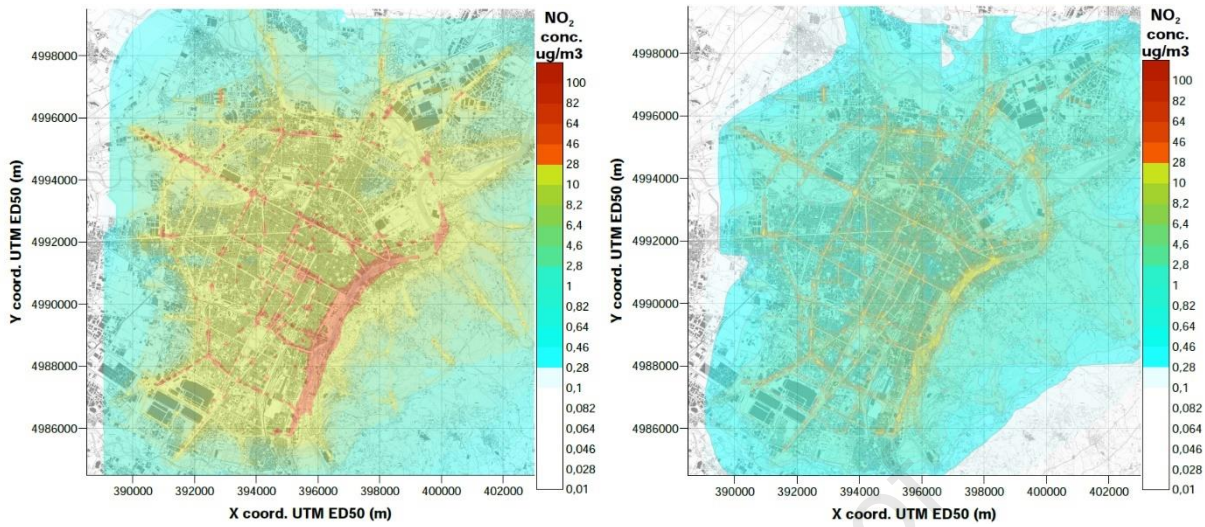

321

322 *Figure 4. Maps of NO_2 concentration in the Turin area generated by road traffic sources during normal days (left)*

323 *and COVID-19 days (right).*

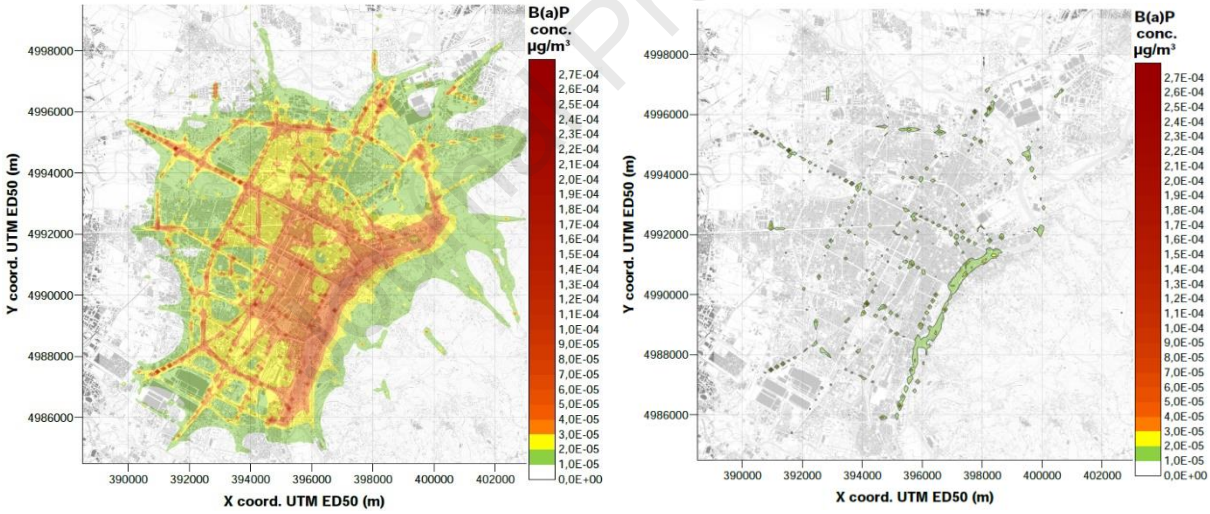

324

325 *Figure 5. Maps of BaP concentration in the Turin area generated by road traffic sources during normal days (left)*

326 *and COVID-19 days (right).*

327

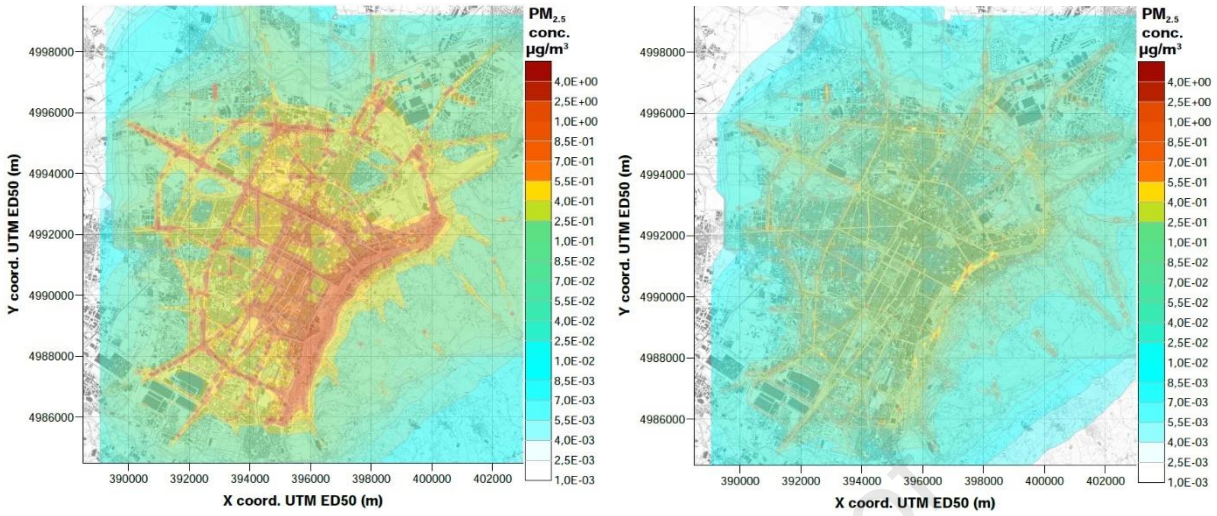

328

329 *Figure 6. Maps of $PM_{2.5}$ concentration in the Turin area generated by road traffic sources during normal days (left)*

330 *and COVID-19 days (right).*

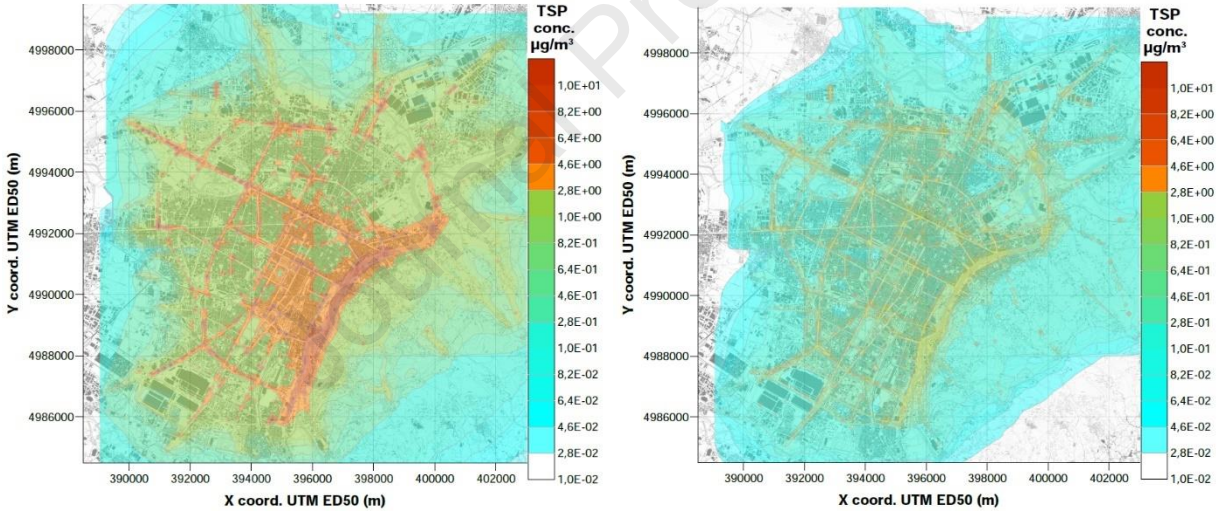

331

332 *Figure 7. Maps of TSP concentration in the Turin area generated by road traffic sources during normal days (left)*

333 *and COVID-19 days (right).*

334

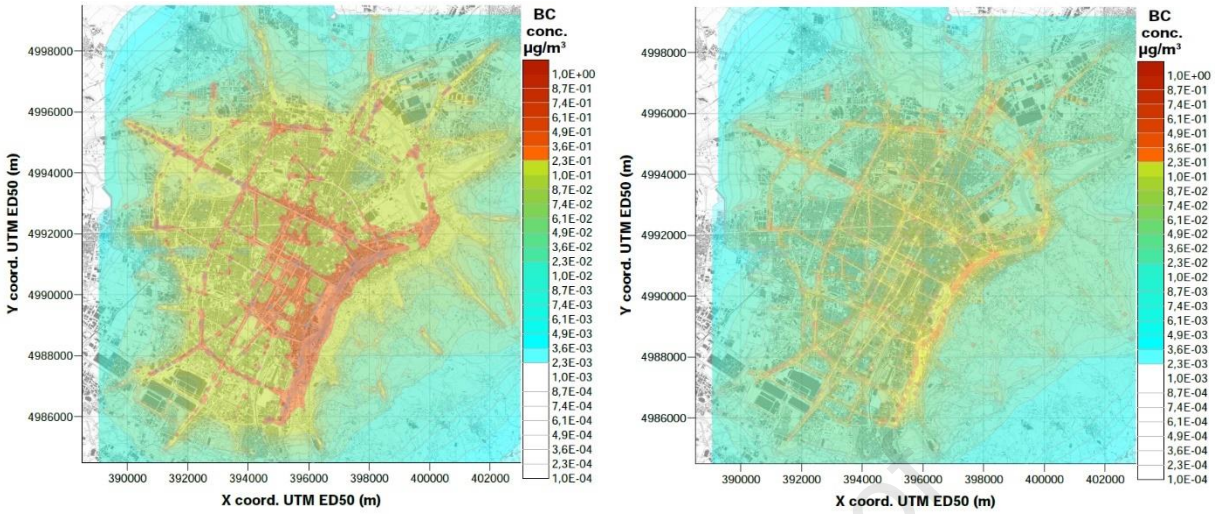

335

336 *Figure 8. Maps of BC concentration in the Turin area generated by road traffic sources during normal days (left)*

337 *and COVID-19 days (right).*

338

339 *Table 2. Pollutant concentration reduction attributed to traffic in the Turin area during COVID-19 days concerning*

340 *normal days.*

Pollutant	Traffic concentration reduction (%)		
	min	mean	max
NO_x	70.7	82.2	87.0
BaP	73.5	83.7	88.1
$PM_{2.5}$	70.0	81.9	86.8
TSP	70.6	82.2	86.9
BC	72.1	83.0	87.9

341

342

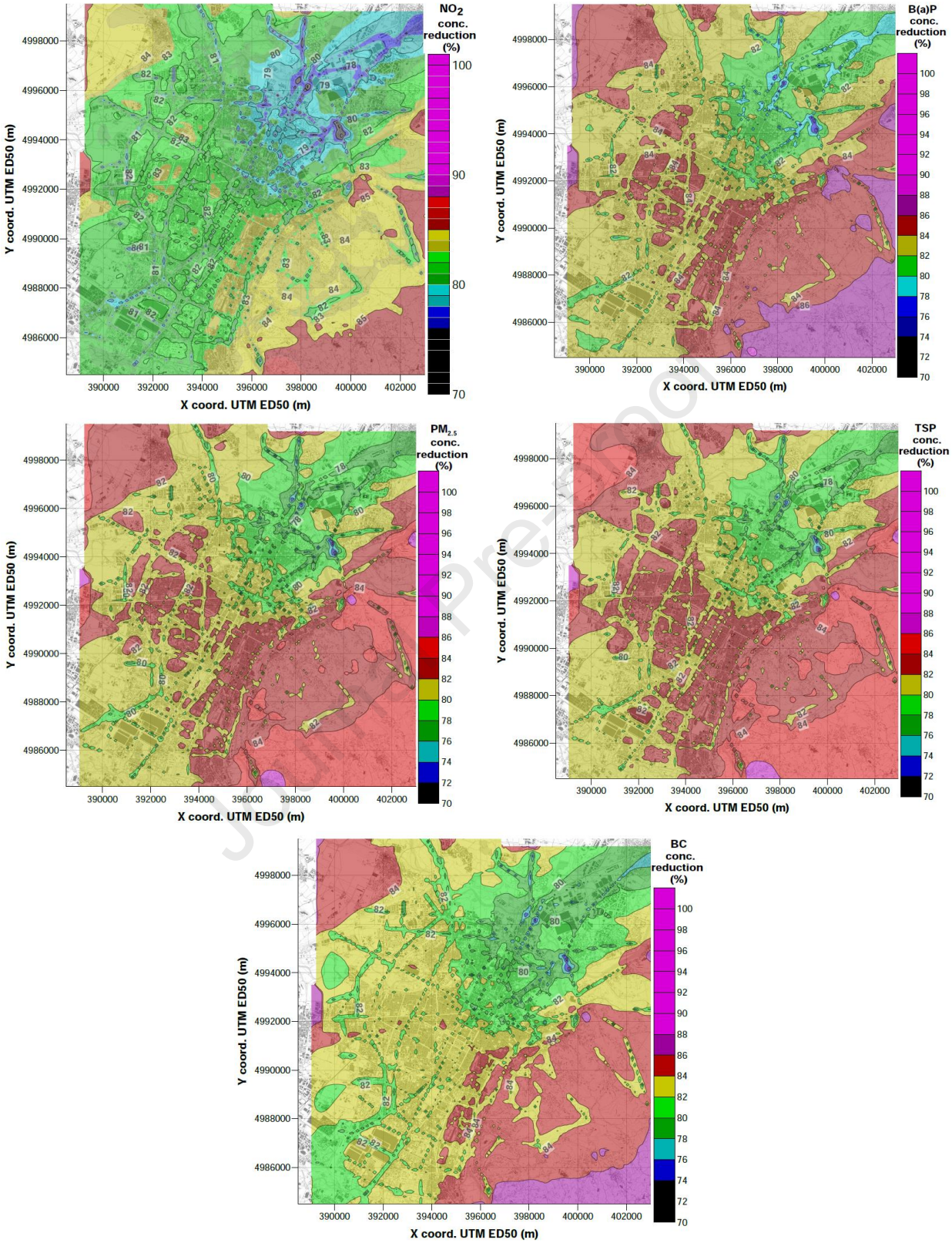

343 *Figure 9. Maps of pollutants concentration reduction during COVID-19 days concerning normal days.*

4. Discussion

The real-time traffic monitoring in Turin during the whole country lockdown period from March 9th to May 18th, 2020, indicated a significant traffic flow reduction in this metropolitan area. Several companies have published periodic mobility reports based on the location data collected through their services, including Google LLC (2020) and TomTom International BV (2020), or have shared their data through analytical platforms, such as Apple Inc. (2020). The data reported in these reports are consistent with the results obtained in our study, all indicating a flow reduction of around 80%. Tables A2 and A3 presented in the Appendix show that traffic flow had a varying reduction depending on the road and hour of the day. Spatial variations are mainly attributed to the road typology. In general, larger roads (e.g. points 15 and 105), which serve as connections between different areas of the city showed lower reductions, while inner roads serving residential areas (e.g. points 39 and 42) showed larger reductions.

The decrease in road mobility resulted in a significant reduction in the emission of the considered pollutants during the studied period in Turin, similar to many other cities in Italy (Gualtieri et al., 2020) and other countries (Chen et al., 2021; Collivignarelli et al., 2021b) reporting significant reductions in the traffic-induced emissions during the lockdown restrictions. Comparing the daily emissions of NO_2, BaP, $PM_{2.5}$, TSP, and BC resulting from the road traffic on normal days and during the COVID-19 lockdown shows that the city experienced more reduction in the emission of air pollutants during non-working days than working days. This difference is mainly due to the activities of some occupations that could not be postponed, canceled, or done from home during the lockdown. Moreover, among the five studied pollutants,

BaP had the highest percentage of reduction, while $PM_{2.5}$ showed the lowest percentage of decrease. Different reduction rates may be associated with the difference of emission factors among vehicle typologies. The reduction of traffic flow observed involved mainly a decrease of passenger cars, as this is the most used vehicle typology (81%). For the pollutants whose emission factors for passenger cars have the same order of magnitude as LDVs and HDVs (e.g. BaP, BC), the emission reduction was higher. Conversely, for the pollutants whose emission factors for LDVs and HDVs are higher than those of passenger cars (e.g. NO_x, $PM_{2.5}$), the emission reduction was lower. Although this aspect should be deepened in future studies on traffic flow analysis, the results confirm that the limitation of mobility with private means is of primary importance for administrations (Shams Esfandabadi et al., 2020). These findings are in line with the results of the research conducted by Collivignarelli et al. (2021b), which reports a significant reduction in the concentration of NO_2 during the lockdown period in London, Milan, and Paris and highlight the importance of rethinking vehicles and urban vehicular traffic.

As illustrated in the maps of the pollutants concentration reduction in Figure 9 and reported in Table 2, BaP and $PM_{2.5}$ also represent the maximum and minimum percentage of reduction, respectively, in terms of concentration. These results show similar trends for all pollutants, with some minor differences. Regarding $PM_{2.5}$, making a comparison between the results obtained and the existing studies on the COVID-19 lockdown period is difficult. This is because only primary $PM_{2.5}$ emissions were considered in this study. Most of the other studies published recently considered aggregated (primary and secondary) aerosol emissions, highlighting the complexity of the interpretation of $PM_{2.5}$ behavior (Le et al., 2020; Rossi et al., 2020). In general, however, traffic flow reduction was highly reflected in nitrous oxides concentration reduction.

Figure 4 to Figure 8 show the spatial distribution of pollutants concentration. The impact is more visible in the proximity of roads, where emissions are generated, but the effects are extended to the whole area. The limited height of sources and the limited dispersion close to the ground are the main factors contributing to the observed trend. These maps also show an uneven distribution of concentration in the area, such that concentrations are higher in the south-eastern part of the town. The presence of a river and reliefs in the eastern part of the city (Figure A1 in Appendix A) contributes to this effect, for two reasons: (1) pollutant dispersion eastwards is limited by the river and reliefs (Ravina et al., 2020a), and (2) traffic is more congested in this area, as the town can only be accessed from north and south. Concentration maps referring to the lockdown period show that the impact, in addition to being reduced, is more limited only to the proximity of the roads. This is an important aspect since consequently, for these pollutants representing a hazard for human health, exposure of the population is limited. Figure 9 shows that the concentration reduction is higher in the north-eastern part of the town. The main reason is that the traffic flow in this area (monitoring points 97, 105, and 107, Table A2 and A3) was less reduced, as mobility in this area is more connected to commercial rather than residential activities.

The simulation results for the pollutant NO_2 were compared with the average yearly concentration recorded in four pollutant monitoring stations located in Turin (Rebaudengo, Lingotto, Rubino, and Via Consolata), during the period 2015-2019 and the COVID-19 lockdown period. These monitoring stations record the total ambient concentration of pollutants, which is the result of multiple sources present in the area, as well as the interactions between chemical species and the atmosphere. The comparison is reported in Figure 10. At the Rebaudengo station, the average observed concentration is 65.5 $\mu g/m^3$ and the simulation model shows a concentration of 41.8 $\mu g/m^3$. The average observed concentration in the Via Consolata station is 45.3 $\mu g/m^3$,

411 while the model reports a value of 29.7 $\mu g/m^3$ for this station. Finally, the Lingotto and the Rubino
412 stations have recorded the average observed concentration of 33.0 $\mu g/m^3$ and 31.8 $\mu g/m^3$,
413 respectively, while the simulated model shows 25.6 $\mu g/m^3$ and 15.4 $\mu g/m^3$ for the two stations,
414 respectively.

415 These results are also comparable with the source apportionment data reported in Piedmont
416 Regional Plan for Air Quality (Piedmont Region, 2018). Source apportionment methodology
417 adopted in this document is based on an integration of modeling and analytical techniques. For the
418 modeling source contribution, the methodology adopted is the 3D sensitivity runs / Brute Force
419 Method - BFM. This method involves the creation of a reference simulation (base case) and a
420 suitable number of sensitivity simulations, one for each emission category to be analyzed. The
421 contribution of each category is calculated by analyzing the differences between the results of the
422 sensitivity simulations and those of the base case. Table 3 shows the source apportionment of NO_2
423 concentrations measured on an annual basis at each of the monitoring stations considered.

424 *Table 3. Source apportionment of NO_2 concentrations measured on an annual basis at each of the monitoring*
425 *stations (Piedmont Region, 2018)*

Torino Rebaudengo		**Torino Consolata**		**Torino Lingotto**		**Torino Rubino**	
Emission category	**Share**	**Emission category**	**Share**	**Emission category**	**Share**	**Emission category**	**Share**
Industry	11.2%	Industry	9.1%	Industry	10.8%	Industry	10.7%
Residential heating	9.0%	Residential heating	9.8%	Residential heating	8.8%	Residential heating	8.7%
Road traffic	74.9%	Road traffic	76.5%	Road traffic	76.2%	Road traffic	76.4%
Agriculture	0.6%	Agriculture	0.7%	Agriculture	0.7%	Agriculture	0.7%
Other	4.3%	Other	3.9%	Other	3.5%	Other	3.5%

426

In this table, the share of traffic sources from the total NO_2 concentration is reported as 74.9% for Rebaudengo station, 76.5% for Via Consolata station, 76.2% for Lingotto station, and 76.4% for Rubino station. In the simulated concentrations, a share of 63.8% is found at the Rebaudengo station (-11.1% with respect to the inventory data), a share of 65.5% is found at Via della Consolata station (-11.0%), a share of 77.8% is found at the Lingotto station (+1.6%), and a share of 48.4% is found at the Rubino station (-28.0%). Therefore, simulated concentrations of road traffic sources show a similar share with respect to the measured total concentration. The difference does not exceed 11.1% for three over four monitoring stations. The only exception is the Rubino station, where concentrations are underestimated, probably because of the influence of the nearby ring road, which was not included in the study.

During the lockdown period, the estimated contribution of traffic emission to the total recorded concentration fell considerably. A share of 22% was found at the Lingotto station, 23% at Via della Consolata station, 31% at Rebaudengo station, and 23% at Rubino station. This reduced share with respect to the normal period, besides the reduced mobility, may also be attributed to the increase of emissions from the residential sector that was confirmed by other studies (Deserti et al., 2020b). Nevertheless, it must be pointed out that the results reported in Figure 10 mainly serve as a piece of indicative information on the validity of the present analysis, which was strictly based on the comparison of primary pollutant emissions, thus does not consider complex aspects of air quality analysis, such as the interaction of multiple emission sources and secondary pollutant transformations.

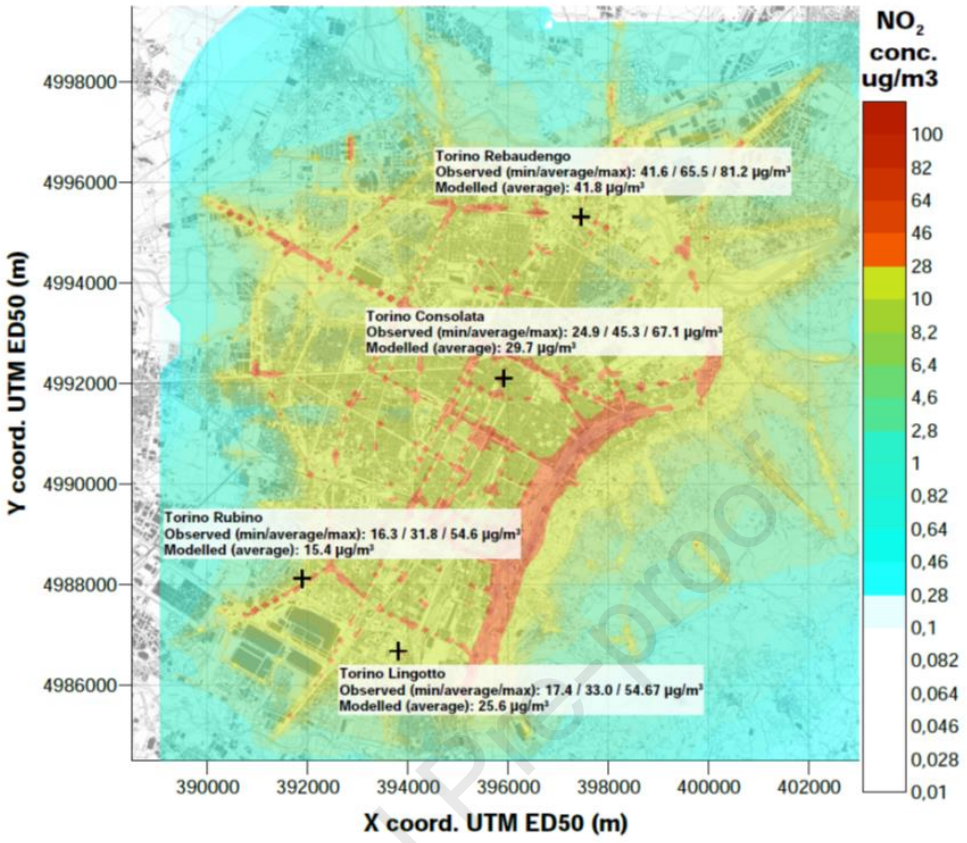
NO2 conc. ug/m3
100
82
64
46
28
10
8,2
6,4
4,6
2,8
1
0,82
0,64
0,46
0,28
0,1
0,082
0,064
0,046
0,028
0,01
Torino Rebaudengo
Observed (min/average/max): 41.6 / 65.5 / 81.2 µg/m³
Modelled (average): 41.8 µg/m³
Torino Consolata
Observed (min/average/max): 24.9 / 45.3 / 67.1 µg/m³
Modelled (average): 29.7 µg/m³
Torino Rubino
Observed (min/average/max): 16.3 / 31.8 / 54.6 µg/m³
Modelled (average): 15.4 µg/m³
Torino Lingotto
Observed (min/average/max): 17.4 / 33.0 / 54.67 µg/m³
Modelled (average): 25.6 µg/m³
Y coord. UTM ED50 (m)
4998000
4996000
4994000
4992000
4990000
4988000
4986000
390000
392000
394000
396000
398000
400000
402000
X coord. UTM ED50 (m)

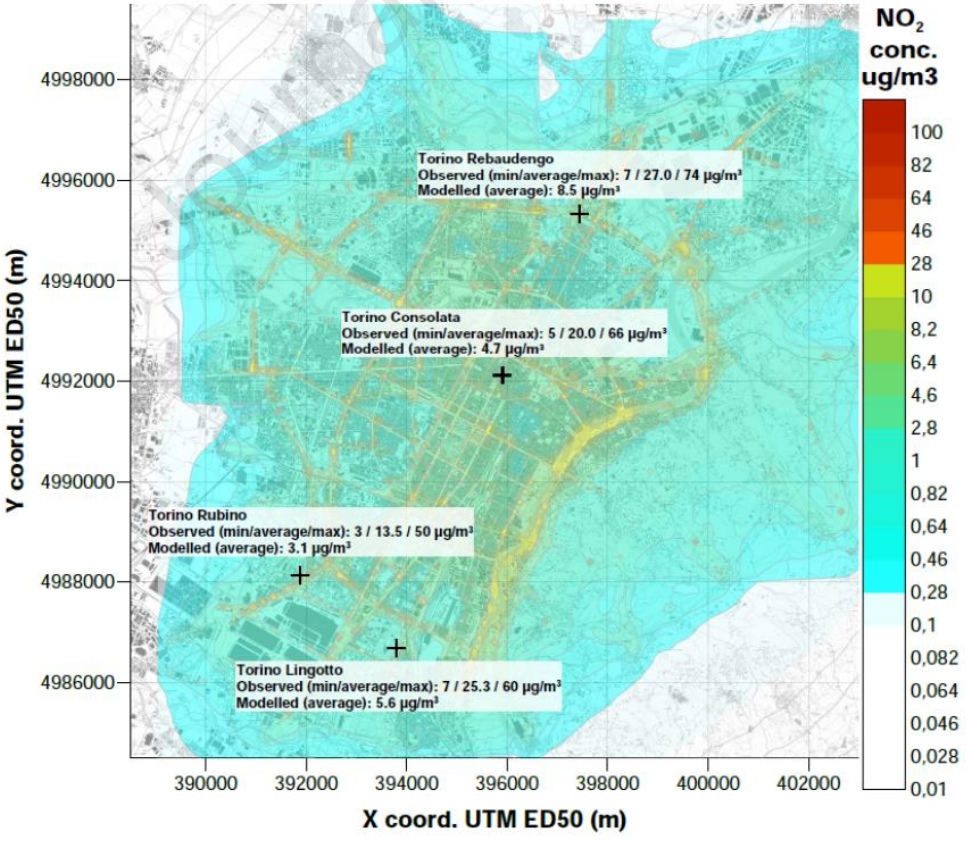
NO2 conc. ug/m3
100
82
64
46
28
10
8,2
6,4
4,6
2,8
1
0,82
0,64
0,46
0,28
0,1
0,082
0,064
0,046
0,028
0,01
Torino Rebaudengo
Observed (min/average/max): 7 / 27.0 / 74 µg/m³
Modelled (average): 8.5 µg/m³
Torino Consolata
Observed (min/average/max): 5 / 20.0 / 66 µg/m³
Modelled (average): 4.7 µg/m³
Torino Rubino
Observed (min/average/max): 3 / 13.5 / 50 µg/m³
Modelled (average): 3.1 µg/m³
Torino Lingotto
Observed (min/average/max): 7 / 25.3 / 60 µg/m³
Modelled (average): 5.6 µg/m³
Y coord. UTM ED50 (m)
4998000
4996000
4994000
4992000
4990000
4988000
4986000
390000
392000
394000
396000
398000
400000
402000
X coord. UTM ED50 (m)

447

448 *Figure 10. Comparison of the model output for NO_2 with the average yearly concentration recorded in four*
449 *pollutant monitoring stations in Turin (Rebaudengo, Lingotto, Rubino, and Via Consolata) in normal days (above)*
450 *and during the COVID-19 lockdown (below).*

451

452 # 5. Conclusion

453 The COVID-19 lockdown period, in its tragic nature, was a unique experience to analyze and
454 confirm the role of traffic emissions in urban areas. However, studies applying real quantification
455 of traffic flows during the pandemic lockdown period are scarce and the literature lacks the
456 application of Lagrangian dispersion models to simulate the dispersion of traffic-induced air
457 pollution during the COVID-19 lockdown.

458 In this research, the effect of the full lockdown period on the reduction of NO_2, BaP, $PM_{2.5}$,
459 TSP, and BC emitted from the road mobile sources, including various types of passenger cars,
460 busses, heavy-duty vehicles, light-duty vehicles, mopeds, and motorcycles in Turin, one of the
461 most polluted cities in Italy, was investigated. To do so, the real-time traffic flow of the city during
462 the first lockdown period of the country was recorded and fed into a Lagrangian dispersion model.
463 In the case study analyzed, it was clear that the reduction in vehicular traffic in Turin significantly
464 contributed to the improvement of air quality during the lockdown days. Studying the emission of
465 pollutants in the city during a one-week period in the full lockdown condition indicated a reduction
466 between 71.4% (referring to $PM_{2.5}$ during the working days) and 85.5% (referring to BaP during
467 non-working days). Furthermore, the reduction in the concentration of pollutants in this period
468 varied between 70% (for $PM_{2.5}$) and 88.1% (for BaP).

In the concluding remarks, it is necessary to report some important considerations regarding the limitations related to the methodology adopted in the present study. The first is that the present study is based only on the dispersion analysis of primary pollutants and does not consider the totality of the sources present in the area under examination and the chemical transformations occurring between the various species. When considering pollutants that do not tend to undergo secondary transformations, the results reported are fully in line with already published studies (Collivignarelli et al., 2020; Xiang et al., 2020). For PM, it should be noted that the reduction obtained refers only to the primary component. As shown in several other studies (Adams, 2020; Huang et al., 2020; Le et al., 2020; Sreekanth et al., 2021), the overall PM trend, also considering the secondary component, has different results due to multiple factors, which are outside the scope of this study. The second limitation of the method is the application of bulk emission factors, due to the lack of sufficiently accurate data of vehicle speed during the COVID-19 lockdown period. It is not possible to quantify to what extent the change in travel speed resulting from the reduction in traffic flow may have affected vehicle emissions. Considering the method applied, it is clear that in the scenarios examined, the reduction in emissions depended mainly on the reduction in traffic flow on the various sections of the road network and the change in the type of vehicles on the road. The results showed that the reduction of emissions, in addition to the renewal of the vehicle fleet, must be mainly linked to the reduction of movements with private means of transport, given that cars are by far the most present type of vehicles on the road. This consideration is particularly important regarding minor pollutants, such as BaP, and BC, which are majorly dangerous for human health.

The subsequent phase of analyzing the spatial distribution of concentrations provided important insights. This research was the first to use a Lagrangian dispersion modeling approach

492 to simulate the dispersion of traffic-induced air pollution during the COVID-19 pandemic. Results
493 showed that in conditions of high vehicular flow, these impacts can extend beyond the proximity
494 of traffic routes and affect pertinential residential areas or parks. On the other hand, a marked
495 reduction in vehicular traffic tends to limit the spatial extension of the impacts. Given the
496 complexity of the subject, these results are recommended to be compared and discussed in future
497 analyses. Confirmation or refutation of these results would bring important implications for air
498 quality and mobility planning in urban areas. Such future studies will bring further knowledge if
499 more detailed and accurate datasets on vehicle flow typology and speed are collected and provided
500 by administrations and stakeholders. Similarly, analyzing different urban areas around the world,
501 in various periods, as well as applying different modeling tools will undoubtedly help increase
502 current knowledge of the topic.

503

504 References

505 5T, Regione_Piemonte, 2019. Report 2017 sulla mobilità veicolare in Piemonte. Torino, Italy.

506 Abdul-Wahab, S., Al-Rawas, G., Ali, S., Fadlallah, S., Al-Dhamri, H., 2017. Atmospheric dispersion
507 modeling of CO2 emissions from a cement plant's sources. Clean Technol. Environ. Policy 19,
508 1621–1638. https://doi.org/10.1007/s10098-017-1352-y

509 Abdul-Wahab, S.A., Fadlallah, S.O., 2014. A study of the effects of vehicle emissions on the atmosphere
510 of Sultan Qaboos University in Oman. Atmos. Environ. 98, 158–167.
511 https://doi.org/10.1016/j.atmosenv.2014.08.049

512 Adams, M.D., 2020. Air pollution in Ontario, Canada during the COVID-19 State of Emergency. Sci.
513 Total Environ. 742, 140516. https://doi.org/10.1016/j.scitotenv.2020.140516

514 Ambade, B., Sankar, T.K., Kumar, A., Gautam, A.S., Gautam, S., 2021. COVID-19 lockdowns reduce
515 the Black carbon and polycyclic aromatic hydrocarbons of the Asian atmosphere: source
516 apportionment and health hazard evaluation. Environ. Dev. Sustain. https://doi.org/10.1007/s10668-
517 020-01167-1

518 Apple Inc., 2020. COVID-19 Mobility Trends Reports [WWW Document]. URL
519 https://covid19.apple.com/mobility (accessed 12.23.20).

520 Bono, R., Romanazzi, V., Bellisario, V., Tassinari, R., Trucco, G., Urbino, A., Cassardo, C., Siniscalco,
521 C., Marchetti, P., Marcon, A., 2016. Air pollution, aeroallergens and admissions to pediatric
522 emergency room for respiratory reasons in Turin, northwestern Italy. BMC Public Health 16, 1–11.
523 https://doi.org/10.1186/s12889-016-3376-3

524 Borge, R., Santiago, J.L., de la Paz, D., Martín, F., Domingo, J., Valdés, C., Sánchez, B., Rivas, E.,
525 Rozas, M.T., Lázaro, S., Pérez, J., Fernández, Á., 2018. Corrigendum to "Application of a short
526 term air quality action plan in Madrid (Spain) under a high-pollution episode - Part II: Assessment
527 from multi-scale modelling" [Sci. Total Environ. 635C (2018) 1575-1585]. Sci. Total Environ. 637–
528 638, 1627. https://doi.org/10.1016/j.scitotenv.2018.05.202

529 Brusca, S., Famoso, F., Lanzafame, R., Mauro, S., Messina, M., Strano, S., 2016. PM10 Dispersion
530 Modeling by Means of CFD 3D and Eulerian–Lagrangian Models: Analysis and Comparison with
531 Experiments. Energy Procedia 101, 329–336. https://doi.org/10.1016/j.egypro.2016.11.042

532 Cai, S., Wang, Y., Zhao, B., Wang, S., Chang, X., Hao, J., 2017. The impact of the "Air Pollution
533 Prevention and Control Action Plan" on PM2.5 concentrations in Jing-Jin-Ji region during 2012–
534 2020. Sci. Total Environ. 580, 197–209. https://doi.org/10.1016/j.scitotenv.2016.11.188

535 Calori, G., Clemente, M., De Maria, R., Finardi, S., Lollobrigida, F., Tinarelli, G., 2006. Air quality
536 integrated modelling in Turin urban area. Environ. Model. Softw. 21, 468–476.
537 https://doi.org/10.1016/j.envsoft.2004.06.009

Cartenì, A., Di Francesco, L., Martino, M., 2020. How mobility habits influenced the spread of the COVID-19 pandemic: Results from the Italian case study. Sci. Total Environ. 741, 140489. https://doi.org/10.1016/j.scitotenv.2020.140489

Cazzolla Gatti, R., Velichevskaya, A., Tateo, A., Amoroso, N., Monaco, A., 2020. Machine learning reveals that prolonged exposure to air pollution is associated with SARS-CoV-2 mortality and infectivity in Italy. Environ. Pollut. 267, 115471. https://doi.org/10.1016/j.envpol.2020.115471

Chakraborty, I., Maity, P., 2020. COVID-19 outbreak: Migration, effects on society, global environment and prevention. Sci. Total Environ. 728, 138882. https://doi.org/10.1016/j.scitotenv.2020.138882

Charabi, Y., Abdul-Wahab, S., Al-Rawas, G., Al-Wardy, M., Fadlallah, S., 2018. Investigating the impact of monsoon season on the dispersion of pollutants emitted from vehicles: A case study of Salalah City, Sultanate of Oman. Transp. Res. Part D Transp. Environ. 59, 108–120. https://doi.org/10.1016/j.trd.2017.12.019

Chen, F., Chen, Z., 2021. Cost of economic growth: Air pollution and health expenditure. Sci. Total Environ. 755, 142543. https://doi.org/10.1016/j.scitotenv.2020.142543

Chen, Z., Hao, X., Zhang, X., Chen, F., 2021. Have traffic restrictions improved air quality? A shock from COVID-19. J. Clean. Prod. 279, 123622. https://doi.org/10.1016/j.jclepro.2020.123622

Collivignarelli, M.C., Abbà, A., Bertanza, G., Pedrazzani, R., Ricciardi, P., Carnevale Miino, M., 2020. Lockdown for CoViD-2019 in Milan: What are the effects on air quality? Sci. Total Environ. 732, 1–9. https://doi.org/10.1016/j.scitotenv.2020.139280

Collivignarelli, M.C., Abbà, A., Caccamo, F.M., Bertanza, G., Pedrazzani, R., Baldi, M., Ricciardi, P., Carnevale Miino, M., 2021a. Can particulate matter be identified as the primary cause of the rapid spread of CoViD-19 in some areas of Northern Italy? Environ. Sci. Pollut. Res. 2. https://doi.org/10.1007/s11356-021-12735-x

Collivignarelli, M.C., De Rose, C., Abbà, A., Baldi, M., Bertanza, G., Pedrazzani, R., Sorlini, S.,

562 Carnevale Miino, M., 2021b. Analysis of lockdown for CoViD-19 impact on NO2 in London, Milan
563 and Paris: What lesson can be learnt? Process Saf. Environ. Prot. 146, 952–960.
564 https://doi.org/10.1016/j.psep.2020.12.029

565 Deserti, M., Raffaelli, K., Ramponi, L., Carbonara, C., Agostini, C., Amorati, R., Arvani, B., Giovannini,
566 G., Maccaferri, S., Poluzzi, V., Stortini, M., Trentini, A., Tugnoli, S., Vasconi, M., 2020a. Covid-19
567 and air quality in the Po Valley. Emilia-Romagna Region, Italy.

568 Deserti, M., Raffaelli, K., Ramponi, L., Carbonara, C., Agostini, C., Amorati, R., Arvani, B., Giovannini,
569 G., Maccaferri, S., Poluzzi, V., Stortini, M., Trentini, A., Tugnoli, S., Vasconi, M., 2020b. Report 2
570 COVID-19 studio preliminare degli effetti delle misure COVID-19 sulle emissioni in atmosfera e
571 sulla qualita dell'aria nel bacino padano. Emilia-Romagna Region, Italy.

572 Dettori, M., Deiana, G., Balletto, G., Borruso, G., Murgante, B., Arghittu, A., Azara, A., Castiglia, P.,
573 2020. Air pollutants and risk of death due to COVID-19 in Italy. Environ. Res. 110459.
574 https://doi.org/10.1016/j.envres.2020.110459

575 EPA, 2015. Guidance on the use of models for assessing the impacts of emissions from single sources on
576 the secondarily formed pollutants ozone and PM2.5.

577 Exponent, 2019. CALPUFF Version 7 Users Guide Addendum. Maynard, USA.

578 Gautam, S., 2020. COVID-19: air pollution remains low as people stay at home. Air Qual. Atmos. Heal.
579 13, 853–857. https://doi.org/10.1007/s11869-020-00842-6

580 Google LLC, 2020. COVID-19 community mobility reports [WWW Document]. URL
581 https://www.google.com/covid19/mobility/ (accessed 12.23.20).

582 Griffith, S.M., Huang, W.-S., Lin, C.-C., Chen, Y.-C., Chang, K.-E., Lin, T.-H., Wang, S.-H., Lin, N.-H.,
583 2020. Long-range air pollution transport in East Asia during the first week of the COVID-19
584 lockdown in China. Sci. Total Environ. 741, 140214.
585 https://doi.org/10.1016/j.scitotenv.2020.140214

586 Gross, P.L., Buchanan, N., Sané, S., 2019. Blue skies in the making: Air quality action plans and urban
587 imaginaries in London, Hong Kong, and San Francisco. Energy Res. Soc. Sci. 48, 85–95.
588 https://doi.org/10.1016/j.erss.2018.09.019

589 Gualtieri, G., Brilli, L., Carotenuto, F., Vagnoli, C., Zaldei, A., Gioli, B., 2020. Quantifying road traffic
590 impact on air quality in urban areas: A Covid19-induced lockdown analysis in Italy. Environ. Pollut.
591 267, 115682. https://doi.org/10.1016/j.envpol.2020.115682

592 Gupta, A., Bherwani, H., Gautam, S., Anjum, S., Musugu, K., Kumar, N., Anshul, A., Kumar, R., 2020.
593 Air pollution aggravating COVID-19 lethality? Exploration in Asian cities using statistical models.
594 Environ. Dev. Sustain. https://doi.org/10.1007/s10668-020-00878-9

595 Guttikunda, S.K., Nishadh, K.A., Gota, S., Singh, P., Chanda, A., Jawahar, P., Asundi, J., 2019. Air
596 quality, emissions, and source contributions analysis for the Greater Bengaluru region of India.
597 Atmos. Pollut. Res. 10, 941–953. https://doi.org/10.1016/j.apr.2019.01.002

598 Holnicki, P., Kałuszko, A., Trapp, W., 2016. An urban scale application and validation of the CALPUFF
599 model. Atmos. Pollut. Res. 7, 393–402. https://doi.org/10.1016/j.apr.2015.10.016

600 Huang, X., Ding, A., Gao, J., Zheng, B., Zhou, D., Qi, X., Tang, R., Wang, J., Ren, C., Nie, W., Chi, X.,
601 Xu, Z., Chen, L., Li, Y., Che, F., Pang, N., Wang, H., Tong, D., Qin, W., Cheng, W., Liu, W., Fu,
602 Q., Liu, B., Chai, F., Davis, S.J., Zhang, Q., He, K., 2020. Enhanced secondary pollution offset
603 reduction of primary emissions during COVID-19 lockdown in China. Natl. Sci. Rev.
604 https://doi.org/10.1093/nsr/nwaa137

605 Izquierdo, R., García Dos Santos, S., Borge, R., Paz, D. de la, Sarigiannis, D., Gotti, A., Boldo, E., 2020.
606 Health impact assessment by the implementation of Madrid City air-quality plan in 2020. Environ.
607 Res. 183, 109021. https://doi.org/10.1016/j.envres.2019.109021

608 Ježek, I., Drinovec, L., Ferrero, L., Carriero, M., Močnik, G., 2015. Determination of car on-road black
609 carbon and particle number emission factors and comparison between mobile and stationary

measurements. Atmos. Meas. Tech. 8, 43–55. https://doi.org/10.5194/amt-8-43-2015

Kesarkar, A.P., Dalvi, M., Kaginalkar, A., Ojha, A., 2007. Coupling of the Weather Research and Forecasting Model with AERMOD for pollutant dispersion modeling. A case study for PM10 dispersion over Pune, India. Atmos. Environ. 41, 1976–1988. https://doi.org/10.1016/j.atmosenv.2006.10.042

Khan, S., Hassan, Q., 2020. Review of Development in Air Quality Modeling and Air Quality Dispersion Models. J. Environ. Eng. Sci. 1–10. https://doi.org/10.1680/jenes.20.00004

Krecl, P., Johansson, C., Targino, A.C., Ström, J., Burman, L., 2017. Trends in black carbon and size-resolved particle number concentrations and vehicle emission factors under real-world conditions. Atmos. Environ. 165, 155–168. https://doi.org/10.1016/j.atmosenv.2017.06.036

Kyoto-Club, 2019. Politiche di Mobilità e Qualita dell'aria nelle 14 Citta e aree Metropolitane 2017-2018. Rome, Italy.

Le, T., Wang, Y., Liu, L., Yang, J., Yung, Y.L., Li, G., Seinfeld, J.H., 2020. Unexpected air pollution with marked emission reductions during the COVID-19 outbreak in China. Science (80-.). 369, 702–706. https://doi.org/10.1126/science.abb7431

Liu, F., Wang, M., Zheng, M., 2021. Effects of COVID-19 lockdown on global air quality and health. Sci. Total Environ. 755, 142533. https://doi.org/10.1016/j.scitotenv.2020.142533

Liu, Y., Zhao, Y., Lu, W., Wang, H., Huang, Q., 2019. ModOdor: 3D numerical model for dispersion simulation of gaseous contaminants from waste treatment facilities. Environ. Model. Softw. 113, 1–19. https://doi.org/10.1016/j.envsoft.2018.12.001

Malandrino, M., Casazza, M., Abollino, O., Minero, C., Maurino, V., 2016. Size resolved metal distribution in the PM matter of the city of Turin (Italy). Chemosphere 147, 477–489. https://doi.org/10.1016/j.chemosphere.2015.12.089

Menut, L., Bessagnet, B., Siour, G., Mailler, S., Pennel, R., Cholakian, A., 2020. Impact of lockdown

measures to combat Covid-19 on air quality over western Europe. Sci. Total Environ. 741, 140426. https://doi.org/10.1016/j.scitotenv.2020.140426

Muhammad, S., Long, X., Salman, M., 2020. COVID-19 pandemic and environmental pollution: A blessing in disguise? Sci. Total Environ. 728, 138820. https://doi.org/10.1016/j.scitotenv.2020.138820

Naeger, A.R., Murphy, K., 2020. Impact of COVID-19 Containment Measures on Air Pollution in California. Aerosol Air Qual. Res. 20, 2025–2034. https://doi.org/10.4209/aaqr.2020.05.0227

Omidi Khaniabadi, Y., Sicard, P., Taiwo, A.M., De Marco, A., Esmaeili, S., Rashidi, R., 2018. Modeling of particulate matter dispersion from a cement plant: Upwind-downwind case study. J. Environ. Chem. Eng. 6, 3104–3110. https://doi.org/10.1016/j.jece.2018.04.022

Padoan, E., Ajmone-Marsan, F., Querol, X., Amato, F., 2018. An empirical model to predict road dust emissions based on pavement and traffic characteristics. Environ. Pollut. 237, 713–720. https://doi.org/10.1016/j.envpol.2017.10.115

Panepinto, D., Brizio, E., Genon, G., 2014. Atmospheric pollutants and air quality effects: limitation costs and environmental advantages (a cost–benefit approach). Clean Technol. Environ. Policy 16, 1805–1813. https://doi.org/10.1007/s10098-014-0727-6

Piedmont Region, 2018. Air Quality Plan [WWW Document]. URL https://www.regione.piemonte.it/web/temi/ambiente-territorio/ambiente/aria/piano-regionale-qualita-dellaria-prqa (accessed 12.24.20).

Pinto, J.A., Kumar, P., Alonso, M.F., Andreão, W.L., Pedruzzi, R., dos Santos, F.S., Moreira, D.M., Albuquerque, T.T. de A., 2020. Traffic data in air quality modeling: A review of key variables, improvements in results, open problems and challenges in current research. Atmos. Pollut. Res. 11, 454–468. https://doi.org/10.1016/j.apr.2019.11.018

Ranjbari, M., Shams Esfandabadi, Z., Zanetti, M.C., Scagnelli, S.D., Siebers, P.-O., Aghbashlo, M., Peng,

W., Quatraro, F., Tabatabaei, M., 2021. Three pillars of sustainability in the wake of COVID-19: A systematic review and future research agenda for sustainable development. J. Clean. Prod. 297, 126660. https://doi.org/10.1016/j.jclepro.2021.126660

Ravina, M., Panepinto, D., Zanetti, M., 2020a. District heating networks: an inter-comparison of environmental indicators. Environ. Sci. Pollut. Res. https://doi.org/10.1007/s11356-020-08734-z

Ravina, M., Panepinto, D., Zanetti, M., 2019. Air Quality Planning and the Minimization of Negative Externalities. Resources 8, 15. https://doi.org/10.3390/resources8010015

Ravina, M., Panepinto, D., Zanetti, M.C., 2020b. Development of the DIDEM Model: Comparative evaluation of CALPUFF and SPRAY dispersion models. Int. J. Environ. Impacts Manag. Mitig. Recover. 3, 1–18. https://doi.org/10.2495/ei-v3-n1-1-18

Ravina, M., Panepinto, D., Zanetti, M.C., 2018. DIDEM - An integrated model for comparative health damage costs calculation of air pollution. Atmos. Environ. 173, 81–95. https://doi.org/10.1016/j.atmosenv.2017.11.010

Rossi, R., Ceccato, R., Gastaldi, M., 2020. Effect of Road Traffic on Air Pollution. Experimental Evidence from COVID-19 Lockdown. Sustainability 12, 8984. https://doi.org/10.3390/su12218984

Saadat, S., Rawtani, D., Hussain, C.M., 2020. Environmental perspective of COVID-19. Sci. Total Environ. 728, 138870. https://doi.org/10.1016/j.scitotenv.2020.138870

Scire, J.S., Lurmann, F.W., Bass, A., Hanna, S.R., 1984. User's guide to the MESOPUFF II model and related processor programs, EPA-600/8–84-013. U.S., Environmental Protection Agency, Research Triangle Park.

Shahbazi, H., Ganjiazad, R., Hosseini, V., Hamedi, M., 2017. Investigating the influence of traffic emission reduction plans on Tehran air quality using WRF/CAMx modeling tools. Transp. Res. Part D Transp. Environ. 57, 484–495. https://doi.org/10.1016/j.trd.2017.08.001

Shahbazi, H., Hosseini, V., 2020. Impact of mobile source emission inventory adjustment on air pollution

photochemical model performance. Urban Clim. 32, 100618. https://doi.org/10.1016/j.uclim.2020.100618

Shams Esfandabadi, Z., Ravina, M., Diana, M., Zanetti, M.C., 2020. Conceptualizing environmental effects of carsharing services: A system thinking approach. Sci. Total Environ. 745, 141169. https://doi.org/10.1016/j.scitotenv.2020.141169

Sharifi, A., Khavarian-Garmsir, A.R., 2020. The COVID-19 pandemic: Impacts on cities and major lessons for urban planning, design, and management. Sci. Total Environ. 749, 142391. https://doi.org/10.1016/j.scitotenv.2020.142391

Shen, L., Zhao, T., Wang, H., Liu, J., Bai, Y., Kong, S., Zheng, H., Zhu, Y., Shu, Z., 2021. Importance of meteorology in air pollution events during the city lockdown for COVID-19 in Hubei Province, Central China. Sci. Total Environ. 754, 142227. https://doi.org/10.1016/j.scitotenv.2020.142227

Sicard, P., De Marco, A., Agathokleous, E., Feng, Z., Xu, X., Paoletti, E., Rodriguez, J.J.D., Calatayud, V., 2020. Amplified ozone pollution in cities during the COVID-19 lockdown. Sci. Total Environ. 735, 139542. https://doi.org/10.1016/j.scitotenv.2020.139542

Sivarethinamohan, R., Sujatha, S., Priya, S., Sankaran, Gafoor, A., Rahman, Z., 2020. Impact of air pollution in health and socio-economic aspects: Review on future approach. Mater. Today Proc. https://doi.org/10.1016/j.matpr.2020.08.540

Son, J.-Y., Fong, K.C., Heo, S., Kim, H., Lim, C.C., Bell, M.L., 2020. Reductions in mortality resulting from reduced air pollution levels due to COVID-19 mitigation measures. Sci. Total Environ. 744, 141012. https://doi.org/10.1016/j.scitotenv.2020.141012

Sreekanth, V., Kushwaha, M., Kulkarni, P., Upadhya, A.R., Spandana, B., Prabhu, V., 2021. Impact of COVID-19 lockdown on the fine particulate matter concentration levels: Results from Bengaluru megacity, India. Adv. Sp. Res. 67, 2140–2150. https://doi.org/10.1016/j.asr.2021.01.017

Stewart, D.R., Saunders, E., Perea, R.A., Fitzgerald, R., Campbell, D.E., Stockwell, W.R., 2017. Linking

706 Air Quality and Human Health Effects Models: An Application to the Los Angeles Air Basin.
707 Environ. Health Insights 11, 1–13. https://doi.org/10.1177/1178630217737551

708 TomTom International BV, 2020. COVID-19 mobility report [WWW Document]. URL
709 https://www.tomtom.com/covid-19/country/italy (accessed 12.23.20).

710 UN, 2015. Resolution adopted by the General Assembly on 25 September 2015.

711 US EPA, 2011. CALPUFF Modeling System Version 6 User Instructions.

712 Wang, Y., Yuan, Y., Wang, Q., Liu, C.G., Zhi, Q., Cao, J., 2020. Changes in air quality related to the
713 control of coronavirus in China: Implications for traffic and industrial emissions. Sci. Total Environ.
714 731, 139133. https://doi.org/10.1016/j.scitotenv.2020.139133

715 WHO, 2020. WHO Director-General's opening remarks at the media briefing on COVID-19 - 11 March
716 2020 [WWW Document]. URL https://www.who.int/director-general/speeches/detail/who-director-
717 general-s-opening-remarks-at-the-media-briefing-on-covid-19---11-march-2020 (accessed 11.9.20).

718 WHO, 2017. Don't Pollute my future! The impact of the environment on children's health, WHO.
719 Geneva, Switzerland.

720 WHO, 2016. Ambient air pollution: A global assessment of exposure and burden of disease. Geneva,
721 Switzerland.

722 WHO, 2005. Air Quality Guidelines- Global Update 2005. Copenhagen, Denmark.

723 Xiang, J., Austin, E., Gould, T., Larson, T., Shirai, J., Liu, Y., Marshall, J., Seto, E., 2020. Impacts of the
724 COVID-19 responses on traffic-related air pollution in a Northwestern US city. Sci. Total Environ.
725 747, 141325. https://doi.org/10.1016/j.scitotenv.2020.141325

726 Zangari, S., Hill, D.T., Charette, A.T., Mirowsky, J.E., 2020. Air quality changes in New York City
727 during the COVID-19 pandemic. Sci. Total Environ. 742, 140496.
728 https://doi.org/10.1016/j.scitotenv.2020.140496

729 Zavala, M., Molina, L.T., Yacovitch, T.I., Fortner, E.C., Roscioli, J.R., Floerchinger, C., Herndon, S.C.,
730 Kolb, C.E., Knighton, W.B., Paramo, V.H., Zirath, S., Mejía, J.A., Jazcilevich, A., 2017. Emission
731 factors of black carbon and co-pollutants from diesel vehicles in Mexico City. Atmos. Chem. Phys.
732 17, 15293–15305. https://doi.org/10.5194/acp-17-15293-2017

733

Appendix A. Supplementary data

Table A1. Vehicle categories, the share of total vehicle flow in Turin, and related average emission factors

Category	Technology	Fuel	Abatement	Share from the total vehicle flow (%)	Emission factors (g/km)				
					NO_x	BaP	$PM_{2.5}$	TSP	BC
1	Buses	Diesel	Urban Buses Standard - Euro V - 2008	0.29%	3.09	9.0E-07	0.046	0.498	0.001
2	Buses	CNG	Urban CNG Buses - EEV	0.04%	2.5	0	0.005	0.163	0
3	Heavy-duty vehicles	Diesel	Diesel 7.5 - 16 t - Conventional	0.46%	8.92	9.0E-07	0.334	0.379	0.205
4	Heavy-duty vehicles	Diesel	Diesel 7.5 - 16 t - Euro I - 91/542/EEC I	0.18%	5.31	9.0E-07	0.201	0.379	0.199
5	Heavy-duty vehicles	Diesel	Diesel 7.5 - 16 t - Euro II - 91/542/EEC II	0.37%	5.5	9.0E-07	0.104	0.379	0.100
6	Heavy-duty vehicles	Diesel	Diesel 7.5 - 16 t - Euro III - 2000	0.55%	4.3	9.0E-07	0.088	0.379	0.090
7	Heavy-duty vehicles	Diesel	Diesel 7.5 - 16 t - Euro IV - 2005	0.67%	2.65	9.0E-07	0.016	0.379	0.016
8	Heavy-duty vehicles	Diesel	Diesel 7.5 - 16 t - Euro V - 2008	0.59%	1.51	9.0E-07	0.016	0.379	0.016
9	Heavy-duty vehicles	Diesel	Diesel 7.5 - 16 t - Euro VI	0.81%	0.291	9.0E-07	0.001	0.379	0.016
10	Light commercial vehicles	Petrol	Diesel - Conventional	0.46%	1.66	2.9E-06	0.179	0.179	0.003
11	Light commercial vehicles	Petrol	Diesel - Euro 1 - 93/59/EEC	0.18%	1.22	6.3E-07	0.117	0.179	0.002
12	Light commercial vehicles	Petrol	Diesel - Euro 2 - 96/69/EEC	0.37%	1.22	6.3E-07	0.117	0.179	0.001
13	Light commercial vehicles	Petrol	Diesel - Euro 3 - 98/69/EC I	0.55%	1.03	6.3E-07	0.078	0.179	0.001
14	Light commercial vehicles	Petrol	Diesel - Euro 4 - 98/69/EC II	0.67%	0.831	6.3E-07	0.041	0.179	0.001
15	Light commercial vehicles	Petrol	Diesel - Euro 5 – EC 715/2007	0.59%	1.15	6.3E-07	0.001	0.179	0.001
16	Light commercial vehicles	Petrol	Diesel - Euro 6 up to 2017	0.81%	0.96	6.3E-07	0.001	0.179	0.001
17	Mopeds and motorcycles	Petrol	2-stroke - Mop - Higher than Euro 3	0.96%	0.25	2.3E-06	0.018	0.091	0.004
18	Mopeds and motorcycles	Petrol	2-stroke - Mop - Euro 3	3.60%	0.25	2.3E-06	0.018	0.091	0.004
19	Mopeds and motorcycles	Petrol	2-stroke - Mop - Euro 2	1.54%	0.25	2.3E-06	0.026	0.091	0.004

20	Mopeds and motorcycles	Petrol	2-stroke - Mop - Euro 1	1.69%	0.25	2.3E-06	0.045	0.091	0.004
21	Mopeds and motorcycles	Petrol	2-stroke - Conventional	3.25%	0.25	2.3E-06	0.091	0.091	0.004
22	Passenger Cars	Diesel	Diesel Medium - Conventional	1.03%	0.546	1.7E-06	0.099	0.099	0.099
23	Passenger Cars	Diesel	Diesel Medium - Euro 1 - 91/441/EEC	0.22%	0.69	1.7E-06	0.084	0.099	0.008
24	Passenger Cars	Diesel	Diesel Medium - Euro 2 - 94/12/EEC	0.84%	0.716	1.7E-06	0.055	0.099	0.042
25	Passenger Cars	Diesel	Diesel Medium - Euro 3 - 98/69/EC I	2.98%	0.773	1.7E-06	0.039	0.099	0.039
26	Passenger Cars	Diesel	Diesel Medium - Euro 4 - 98/69/EC II	6.01%	0.58	1.7E-06	0.031	0.099	0.012
27	Passenger Cars	Diesel	Diesel Medium - Euro 5 – EC 715/2007	6.14%	0.55	1.7E-06	0.002	0.099	0.011
28	Passenger Cars	Diesel	Diesel Medium - Euro 6 up to 2016	11.09%	0.45	1.7E-06	0.002	0.099	0.000
29	Passenger Cars	LPG	LPG - Conventional	0.39%	2.36	1.0E-08	0.002	0.033	0.001
30	Passenger Cars	LPG	LPG - Euro 1 - 91/441/EEC	0.11%	0.414	1.0E-08	0.002	0.033	0
31	Passenger Cars	LPG	LPG - Euro 2 - 94/12/EEC	0.35%	0.18	1.0E-08	0.002	0.033	0
32	Passenger Cars	LPG	LPG - Euro 3 - 98/69/EC I	0.32%	0.09	1.0E-08	0.001	0.033	0
33	Passenger Cars	LPG	LPG - Euro 4 - 98/69/EC II	3.27%	0.056	1.0E-08	0.001	0.033	0
34	Passenger Cars	LPG	LPG - Euro 5 – EC 715/2007	1.85%	0.056	1.0E-08	0.001	0.033	0
35	Passenger Cars	LPG	LPG - Euro 6 – EC 715/2007	3.82%	0.056	1.0E-08	0.001	0.033	0
36	Passenger Cars	Petrol	Petrol Medium - ECE 15/04	5.67%	2.66	4.8E-07	0.002	0.035	0.002
37	Passenger Cars	Petrol	Petrol Medium - Euro 1 - 91/441/EEC	1.11%	0.485	3.2E-07	0.002	0.035	0.002
38	Passenger Cars	Petrol	Petrol Medium - Euro 2 - 94/12/EEC	4.03%	0.255	3.2E-07	0.002	0.035	0.002
39	Passenger Cars	Petrol	Petrol Medium - Euro 3 - 98/69/EC I	4.79%	0.097	3.2E-07	0.001	0.035	0.001
40	Passenger Cars	Petrol	Petrol Medium - Euro 4 - 98/69/EC II	10.02%	0.061	3.2E-07	0.001	0.035	0.001
41	Passenger Cars	Petrol	Petrol Medium - Euro 5 – EC 715/2007	4.86%	0.061	3.2E-07	0.001	0.035	0.001
42	Passenger Cars	Petrol	Petrol Medium - Euro 6 up to 2016	11.33%	0.061	3.2E-07	0.001	0.035	0.001
43	Buses	Electricity		0.01%	0	0.0E+00	0.000	0.154	0
44	Passenger Cars	Electricity		1.15%	0	0.0E+00	0.000	0.033	0

Table A2. Traffic flow reduction in the traffic monitoring points (working days).

Hour of the day	Point ID	15	19	22	26	35	39	42	44	49	56	66	86	97	105	107	Mean	Std. dev.
	Coord. (N, W)	45.0326, 7.6466	45.0364, 7.6966	45.0413, 7.6477	45.0463, 7.6343	45.0527, 7.6347	45.0550, 7.6717	45.0553, 7.6711	45.0555, 7.6720	45.0593, 7.6631	45.0645, 7.6498	45.0702, 7.6940	45.0780, 7.6797	45.0887, 7.6885	45.1045, 7.7015	45.1090, 7.7049		
00:00 – 00:59		92%	90%	100%	95%	93%	100%	100%	100%	95%	100%	100%	100%	93%	89%	90%	**96%**	4%
1:00 – 01:59		100%	90%	100%	90%	85%	100%	100%	100%	100%	100%	100%	100%	85%	92%	91%	**96%**	6%
2:00 – 02:59		100%	89%	100%	100%	100%	100%	100%	100%	100%	100%	100%	100%	72%	87%	86%	**96%**	8%
3:00 – 03:59		100%	79%	100%	82%	100%	100%	100%	100%	100%	100%	100%	100%	100%	80%	82%	**95%**	9%
4:00 – 04:59		64%	80%	100%	76%	84%	100%	100%	71%	100%	100%	100%	100%	73%	67%	78%	**86%**	14%
5:00 – 05:59		44%	60%	86%	71%	72%	67%	75%	71%	86%	70%	72%	76%	71%	60%	76%	**70%**	10%
6:00 – 06:59		48%	60%	76%	68%	59%	67%	76%	72%	76%	68%	65%	68%	64%	60%	63%	**66%**	7%
7:00 – 07:59		34%	75%	85%	81%	77%	76%	79%	83%	84%	80%	76%	75%	77%	73%	73%	**75%**	12%
8:00 – 08:59		55%	74%	78%	80%	75%	78%	78%	74%	83%	74%	77%	73%	74%	73%	76%	**75%**	6%
9:00 – 09:59		60%	77%	80%	79%	71%	80%	78%	77%	81%	77%	80%	79%	77%	72%	77%	**76%**	5%
10:00 – 10:59		57%	73%	82%	77%	66%	79%	77%	77%	79%	77%	77%	78%	75%	71%	71%	**74%**	6%
11:00 – 11:59		61%	74%	84%	76%	65%	77%	77%	77%	75%	75%	76%	78%	73%	69%	70%	**74%**	5%
12:00 – 12:59		55%	73%	84%	75%	66%	77%	73%	77%	72%	77%	75%	77%	70%	69%	69%	**73%**	6%
13:00 – 13:59		51%	72%	81%	74%	66%	77%	75%	75%	71%	74%	77%	75%	70%	68%	68%	**72%**	7%
14:00 – 14:59		57%	76%	81%	74%	68%	79%	78%	81%	79%	79%	77%	79%	74%	72%	70%	**75%**	6%
15:00 – 15:59		60%	77%	83%	77%	71%	80%	79%	82%	80%	80%	80%	80%	76%	73%	73%	**77%**	6%
16:00 – 16:59		65%	76%	86%	79%	74%	84%	83%	83%	78%	82%	82%	82%	76%	73%	76%	**79%**	5%
17:00 – 17:59		71%	77%	85%	78%	74%	84%	82%	84%	77%	83%	79%	80%	76%	74%	78%	**79%**	4%
18:00 – 18:59		77%	80%	87%	82%	78%	83%	84%	85%	76%	83%	82%	81%	77%	77%	81%	**81%**	3%
19:00 – 19:59		74%	84%	87%	85%	82%	87%	83%	89%	81%	85%	84%	86%	79%	81%	84%	**83%**	4%
20:00 – 20:59		76%	86%	92%	85%	81%	88%	86%	89%	87%	86%	85%	90%	82%	85%	82%	**85%**	4%
21:00 – 21:59		76%	85%	92%	86%	80%	85%	86%	85%	85%	84%	90%	89%	82%	82%	81%	**84%**	4%
22:00 – 22:59		79%	89%	92%	85%	82%	91%	90%	94%	87%	91%	89%	91%	84%	83%	79%	**87%**	5%
23:00 – 00:59		90%	90%	96%	92%	89%	96%	96%	93%	94%	95%	94%	95%	91%	85%	91%	**92%**	3%
Average		**69%**	**78%**	**88%**	**81%**	**77%**	**85%**	**85%**	**84%**	**84%**	**84%**	**84%**	**85%**	**78%**	**76%**	**78%**	**81%**	5%
Std. dev.		18%	8%	8%	8%	11%	10%	9%	10%	9%	10%	10%	10%	8%	9%	8%		

Table A3. Traffic flow reduction in the traffic monitoring points (non-working days).

Hour of the day	Point ID	15	19	22	26	35	39	42	44	49	56	66	86	97	105	107	Mean	Std. dev.
	Coord.	45.0326, 7.6466	45.0364, 7.6966	45.0413, 7.6477	45.0463, 7.6943	45.0527, 7.6947	45.0550, 7.6717	45.0553, 7.6711	45.0555, 7.6720	45.0593, 7.6631	45.0645, 7.6498	45.0702, 7.6940	45.0780, 7.6797	45.0887, 7.6885	45.1045, 7.7015	45.1090, 7.7049		
00:00 – 00:59		94%	96%	100%	97%	97%	100%	100%	100%	100%	100%	100%	98%	96%	93%	97%	**98%**	2%
1:00 – 01:59		100%	97%	100%	100%	100%	100%	100%	100%	100%	100%	100%	100%	95%	97%	97%	**99%**	2%
2:00 – 02:59		100%	96%	100%	100%	100%	100%	100%	100%	100%	100%	100%	100%	100%	95%	96%	**99%**	2%
3:00 – 03:59		100%	94%	100%	96%	100%	100%	100%	100%	100%	100%	100%	100%	100%	94%	94%	**99%**	2%
4:00 – 04:59		100%	91%	100%	100%	100%	100%	100%	100%	100%	100%	100%	100%	100%	82%	100%	**98%**	5%
5:00 – 05:59		48%	61%	93%	59%	50%	84%	100%	71%	83%	80%	79%	84%	78%	72%	72%	**74%**	14%
6:00 – 06:59		0%	35%	71%	45%	15%	49%	80%	71%	71%	55%	45%	47%	55%	41%	56%	**49%**	21%
7:00 – 07:59		35%	51%	80%	63%	51%	72%	47%	77%	55%	61%	65%	45%	68%	51%	49%	**58%**	12%
8:00 – 08:59		58%	68%	82%	75%	69%	74%	76%	82%	72%	68%	67%	73%	76%	67%	71%	**72%**	6%
9:00 – 09:59		64%	78%	93%	85%	78%	79%	78%	77%	82%	80%	80%	84%	84%	80%	80%	**80%**	6%
10:00 – 10:59		75%	80%	93%	85%	79%	84%	78%	88%	85%	86%	86%	87%	85%	82%	85%	**84%**	4%
11:00 – 11:59		78%	85%	91%	85%	79%	81%	78%	85%	82%	80%	81%	86%	81%	85%	84%	**83%**	3%
12:00 – 12:59		76%	86%	91%	84%	81%	82%	82%	86%	81%	81%	85%	86%	81%	85%	82%	**83%**	3%
13:00 – 13:59		61%	82%	88%	78%	70%	79%	77%	82%	72%	78%	76%	81%	71%	80%	72%	**77%**	6%
14:00 – 14:59		54%	77%	90%	79%	71%	79%	80%	88%	80%	80%	81%	85%	75%	80%	79%	**79%**	8%
15:00 – 15:59		80%	84%	92%	88%	77%	87%	84%	88%	88%	86%	89%	91%	83%	88%	85%	**86%**	4%
16:00 – 16:59		85%	90%	92%	87%	82%	88%	90%	89%	91%	87%	90%	93%	85%	87%	88%	**88%**	3%
17:00 – 17:59		87%	90%	92%	86%	78%	87%	88%	92%	90%	87%	89%	93%	85%	88%	89%	**88%**	4%
18:00 – 18:59		86%	90%	93%	87%	81%	87%	88%	91%	91%	87%	88%	92%	84%	89%	89%	**88%**	3%
19:00 – 19:59		85%	91%	94%	85%	81%	87%	88%	90%	87%	87%	87%	92%	84%	90%	88%	**88%**	3%
20:00 – 20:59		81%	89%	94%	85%	80%	87%	85%	88%	86%	82%	84%	91%	82%	90%	85%	**86%**	4%
21:00 – 21:59		78%	87%	91%	85%	79%	81%	85%	89%	83%	81%	88%	90%	83%	89%	81%	**85%**	4%
22:00 – 22:59		75%	89%	93%	86%	84%	84%	90%	94%	89%	89%	94%	91%	82%	87%	85%	**87%**	5%
23:00 – 00:59		87%	92%	98%	94%	87%	94%	95%	92%	93%	94%	93%	94%	90%	91%	90%	**92%**	3%
Average		**74%**	**82%**	**92%**	**84%**	**78%**	**85%**	**86%**	**88%**	**86%**	**85%**	**85%**	**87%**	**83%**	**83%**	**83%**	**84%**	4%
Std. dev.		23%	15%	7%	13%	19%	11%	12%	9%	11%	12%	13%	14%	11%	13%	12%		

Table A4. Setting of dispersion simulation parameters.

Parameter	Description	Setting
MGAUSS	Vertical distribution used in the near field	Gaussian
MCTADJ	Terrain adjustment method	Partial plume path adjustment
MSPLIT	Puff splitting	allowed
MCHEM	Chemical mechanism	Transformation rates computed internally (MESOPUFF II scheme)
MDRY	Dry deposition modeled	Not modelled
MDISP	Method used to compute dispersion coefficients	Dispersion coefficients from internally calculated sigma v, sigma w using micrometeorological variables (u*, w*, L, etc.)
MTAULY	Method used for Lagrangian timescale for Sigma-y	Draxler default 617.284 (s)
MCTURB	Method used to compute turbulence sigma-v & sigma-w using micrometeorological variables	Standard CALPUFF subroutines
MBCON	Boundary conditions (concentration)	Not modelled

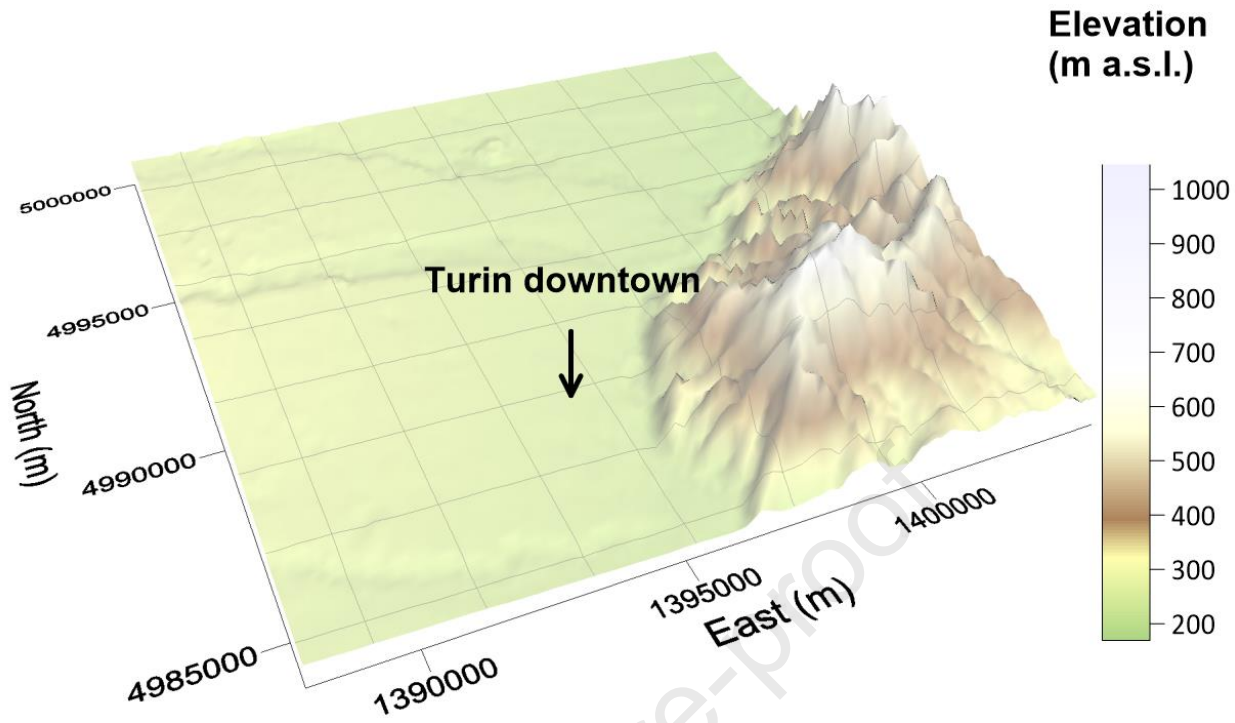

Figure A1. Topography of the modelling domain.